MAY 2 0 1962 UNCLASSIFIED ~~CONFIDENTIAL~~ Copy 29 NASA TM X-691

NASA TM X-691

GROUP 4
Downgraded at 3 year intervals;
declassified after 12 years

Stamped by auth NASA ltr Sta Rev. 12, 1965, s/John T. Sherwood for H. L. Morris. KMC 1-2-66

CLASSIFICATION CHANGED
UNCLASSIFIED
By authority of CSTAR Date 12/31/70
V. 8 No. 74 Bem 3/11/71

# TECHNICAL MEMORANDUM

X-691

## TRANSONIC LONGITUDINAL AND LATERAL AERODYNAMIC CHARACTERISTICS OF A PRELIMINARY CONCEPT OF A FIRST-STAGE HORIZONTAL-TAKE-OFF-AND-HORIZONTAL-LANDING RECOVERABLE BOOSTER WITH A 70° DELTA WING

By P. Kenneth Pierpont

Langley Research Center
Langley Station, Hampton, Va.

CLASSIFIED DOCUMENT - TITLE UNCLASSIFIED

This material contains information affecting the national defense of the United States within the meaning of the espionage laws, Title 18, U.S.C., Secs. 793 and 794, the transmission or revelation of which in any manner to an unauthorized person is prohibited by law.

NATIONAL AERONAUTICS AND SPACE ADMINISTRATION

WASHINGTON May 1962

~~CONFIDENTIAL~~
UNCLASSIFIED

UNCLASSIFIED

~~CONFIDENTIAL~~

NATIONAL AERONAUTICS AND SPACE ADMINISTRATION

TECHNICAL MEMORANDUM X-691

# TRANSONIC LONGITUDINAL AND LATERAL AERODYNAMIC CHARACTERISTICS OF A PRELIMINARY CONCEPT OF A FIRST-STAGE HORIZONTAL-TAKE-OFF-AND-HORIZONTAL-LANDING RECOVERABLE BOOSTER WITH A 70° DELTA WING*

CLASSIFICATION CHANGED
UNCLASSIFIED
To .....
By authority of STAR Date 2/3/70
V. 8, No. 24
Blm 3-11-71

By P. Kenneth Pierpont

SUMMARY

Longitudinal and lateral stability characteristics have been determined for several wing sections and wing-position arrangements of a preliminary configuration for a first-stage horizontal-take-off-and-horizontal-landing recoverable booster in the Langley 8-foot transonic pressure tunnel. The models tested had 70° delta wings with symmetrical and unsymmetrical wedge-slab sections of 2-percent maximum thickness. The semicylindrical fuselage was tested with both high-wing and low-wing arrangements. Data were obtained at 0° and 5° sideslip over an angle-of-attack range from -2° to 14°. Test Reynolds number per foot varied from $1.6 \times 10^6$ to $4.2 \times 10^6$ and Mach numbers ranged from 0.6 to 1.2.

The results showed that approximately equal increments in pitching moment resulted from progressively changing the wing section from a flat-bottom to a symmetrical section, and finally to a flat-top section. Negative pitching-moment increments also resulted from changing from a high-wing to a low-wing arrangement. Longitudinal stability was generally unaffected by either the wing section or the wing-fuselage arrangement. Increases in lift-drag ratio, up to 1.2, resulted from changing the wing section from flat top to flat bottom, but neither the high-wing nor low-wing arrangements affected lift-drag-ratio characteristics. No significant changes in lateral-directional stability were attributed to either wing-section change or wing-fuselage arrangement.

*Title, Unclassified.

UNCLASSIFIED

~~CONFIDENTIAL~~

## INTRODUCTION

A program has been initiated to investigate the aerodynamic characteristics of multistage recoverable boosters at transonic and hypersonic speeds. Results of transonic investigations of a vertical-take-off-and-horizontal-landing (VTOHL) booster configuration with other stages arranged in tandem have been reported in reference 1. An alternate approach to the recoverable-booster problem consists of the utilization of a manned horizontal-take-off-and-horizontal-landing recoverable-booster (HTOHL) configuration with the upper stages arranged in parallel with the first stage.

The present investigation was made to determine the transonic characteristics of a first-stage horizontal-take-off-and-horizontal-landing recoverable booster concept. The model consisted of a delta wing in combination with a body and tail and was approximately 1/50 scale. The configuration was conceived to use advanced turboramjet power plants for which all the hydrocarbon fuel was considered to be carried within the fuselage. Specifications required a maximum of 30,000 pounds of spacecraft weight to be boosted into a 300-nautical-mile orbit from first-stage separation at $M = 6.0$ at about 100,000 feet. Take-off wing loading was assumed to be 120 pounds per square foot and the thrust-weight ratio to be 0.60. The landing wing loading of the first stage alone was found to be about 40 pounds per square foot. The model used for the first stage was identical to the hypersonic cruise vehicle of reference 2.

The tests were made in the Langley 8-foot transonic pressure tunnel over a Mach number range from 0.6 to 1.2 and an angle-of-attack range from $-2^{\circ}$ to $14^{\circ}$ at sideslip angles of $0^{\circ}$ and $5^{\circ}$. Reynolds numbers for the test varied from about $1.6 \times 10^{6}$ to $4.2 \times 10^{6}$ per foot.

## MODEL DESCRIPTION

The model of the first-stage recoverable booster consisted of a $70^{\circ}$ delta wing mounted on a semicylindrical fuselage with an ogival forebody (fig. 1). Photographs of the complete model are shown in figure 2, and the model dimensions are given in table I. No inlets or propulsion nacelles were incorporated into this preliminary configuration. The fuselage length (33 in.) was identical to the root chord of the wing. The fuselage consisted of a semicircular section 6.0 diameters long and an ogival forebody 7.0 diameters long. A table of ordinates for the fuselage forebody is given in figure 1. The surface of the fuselage was shaped to fit each wing configuration. The fuselage volume

was estimated to be approximately that required if hydrocarbon fuels were used for turboramjet propulsion. No fuel was considered to be carried in the wings because of the temperature problem.

The model was arranged so that results for either a high-wing or a low-wing configuration could be obtained by simply testing through a complete positive and negative angle-of-attack range. (See fig. 1.) Two interchangeable wings were constructed so that each could be mounted either upright or inverted on the fuselage. Each wing had a delta planform with 70° leading-edge sweep. The thickness rearward of the 40-percent-chord station was constant and equal to 2 percent of the chord; the trailing edge was blunt. One of the wings had a symmetrical wedge forward of the 40-percent-chord station and the other wing was unsymmetrical with one surface flat from the leading edge to the trailing edge. The leading-edge radius was 0.012 inch for both wings. Three wing sections were thus available: symmetrical, flat bottom, and flat top.

L
1
9
7
5

The vertical fin (fig. 1) could be mounted either on the wing side for the high-wing arrangement or on the fuselage side for the low-wing arrangement as shown in figure 1. The planform of the vertical fin was a half-delta with 70° of leading-edge sweep. The fin had symmetrical wedge-slab sections with 2-percent thickness rearward of the 40-percent-chord station and a blunt trailing edge.

## SYMBOLS

The results of the investigation are presented in coefficient and parameter form. The longitudinal data are referred to the stability axes and the lateral data to the body axes. The moment reference was at $0.25\bar{c}$ which was 16.50 inches forward of the model base and in the plane of symmetry of the wing.

$C_L$ lift coefficient, $\frac{\text{Lift}}{qS}$

$C_D$ drag coefficient, $\frac{\text{Drag}}{qS}$

$C_m$ pitching-moment coefficient about $0.25\bar{c}$, $\frac{\text{Pitching moment}}{qS\bar{c}}$

$C_l$ rolling-moment coefficient, $\frac{\text{Rolling moment}}{qSb}$

| | |
|---|---|
| $C_n$ | yawing-moment coefficient, $\frac{\text{Yawing moment}}{qSb}$ |
| $C_Y$ | side-force coefficient, $\frac{\text{Side force}}{qS}$ |
| $C_{L_\alpha}$ | lift-curve slope, $\partial C_L/\partial\alpha$, per deg |
| $C_{m_{C_L}}$ | longitudinal-stability parameter, $\partial C_m/\partial C_L$ |
| $\partial C_D/\partial C_L^2$ | drag-due-to-lift factor |
| $C_{l_\beta}$ | effective-dihedral parameter, $\Delta C_l/\Delta\beta$, per deg |
| $C_{n_\beta}$ | directional-stability parameter, $\Delta C_n/\Delta\beta$, per deg |
| $C_{Y_\beta}$ | side-force parameter, $\Delta C_Y/\Delta\beta$, per deg |
| L/D | lift-drag ratio, $C_L/C_D$ |
| b | wing span, in. |
| c | chord, in. |
| $\bar{c}$ | mean aerodynamic chord, based on total wing area, in. |
| M | free-stream Mach number |
| q | free-stream dynamic pressure, lb/sq ft |
| R | Reynolds number per foot |
| S | wing area, sq ft |
| x | distance measured from leading edge, in. |
| $\frac{x_{ac}}{\bar{c}}$ | aerodynamic-center location |

$\alpha$ angle of attack, deg

$\beta$ angle of sideslip, deg

Subscripts:

b at model base

o at zero lift

max maximum

L
1
9
7
5

## APPARATUS AND TESTS

The tests were made in the Langley 8-foot transonic pressure tunnel over a range of Mach numbers from 0.6 to 1.2 and a range of angles of attack from $-2^{\circ}$ to $14^{\circ}$ at $0^{\circ}$ and $5^{\circ}$ sideslip. The range of test Reynolds number per foot is shown in figure 3 to vary from $1.6 \times 10^{6}$ to $4.2 \times 10^{6}$. Boundary-layer transition was fixed by a 0.10-inch-wide band of No. 80 carborundum grains (0.008-inch-diameter grit) located at the 5-percent-chord station on all surfaces, including the fuselage forebody. Reference 3 indicates that this size of grain was sufficient to cause transition.

Six-component force and moment data were obtained by means of an internally mounted strain-gage balance. Angles of attack and sideslip were corrected to include balance and sting deflections under load. The axial force was corrected to correspond to a base pressure (acting on the fuselage base together with that portion of the wing base intercepted by the fuselage) equal to the free-stream pressure.

The accuracy of the data has been estimated on the basis of repeatability of data and balance accuracy to be approximately as follows:

| | |
|---|---|
| M | ±0.005 |
| $\alpha$, deg | ±0.1 |
| $\beta$, deg | ±0.1 |
| $C_L$ | ±0.005 |
| $C_D$ | ±0.001 |
| $C_m$ | ±0.002 |
| $C_l$ | ±0.001 |
| $C_n$ | ±0.001 |
| $C_Y$ | ±0.002 |

## PRESENTATION OF RESULTS

The data and summary figures are presented as follows:

| | Figure |
|---|---|
| Aerodynamic characteristics of the high-wing arrangement with the flat-top wing without and with vertical tail. $\beta = 0^{\circ}$ . . . | 4 |
| Aerodynamic characteristics of the low-wing arrangement with the flat-bottom wing without and with vertical tail. $\beta = 0^{\circ}$ . . . . . | 5 |
| Effect of wing section on the aerodynamic characteristics of the high-wing arrangement. $\beta = 0^{\circ}$ . . . . . | 6 |
| Effect of wing section on the aerodynamic characteristics of the low-wing arrangement. $\beta = 0^{\circ}$ . . . . . | 7 |
| Aerodynamic characteristics of the high-wing arrangement with flat-top wing at $5^{\circ}$ of sideslip . . . . . | 8 |
| Effect of wing section on the aerodynamic characteristics of the low-wing arrangement at $5^{\circ}$ of sideslip . . . . . | 9 |
| Effect of wing section and wing arrangement on the longitudinal-stability and drag parameters . . . . . | 10 |
| Effect of wing section and wing arrangement on the variation of aerodynamic-center location with Mach number . . . . . | 11 |
| Effect of wing section and wing arrangement on the variation of L/D with lift coefficient . . . . . | 12 |
| Effect of wing section and wing arrangement on the variation of $(L/D)_{max}$ with Mach number . . . . . | 13 |
| Effect of wing section and wing arrangement on the variation of lift coefficient for $(L/D)_{max}$ with Mach number . . . . . | 14 |
| Effect of angle of attack on the variation of the lateral-directional-stability parameters with Mach number for the high-wing arrangement with flat-top wing . . . . . | 15 |
| Effect of wing section and angle of attack on the variation of the lateral-directional-stability parameters with Mach number for the low-wing arrangement . . . . . | 16 |

## DISCUSSION OF RESULTS

The effects of wing section on the longitudinal aerodynamic characteristics for the high-wing and low-wing arrangements are shown in figures 6 and 7, respectively. A substantial positive shift in $C_{m,o}$ is shown for the flat-top wing section compared with the flat-bottom wing section; this shift is attributable to the change from positive to negative camber. For the low-wing arrangement, figure 7 shows that

approximately equal increments in $C_{m,o}$ (about 0.005) resulted from progressively changing from the flat bottom, to the symmetrical, and finally to the flat-top wing section. For the high-wing arrangement, figure 6 shows approximately the same changes for the flat-top and flat-bottom sections. Comparison of the two figures shows that changing from a high-wing to a low-wing arrangement caused a change in $C_{m,o}$ of about 0.004; hence, the fuselage contributed about one-half of the total increment, or about 0.002. Figure 10 shows that neither the wing section nor the wing-fuselage arrangement caused any significant change in the values of the longitudinal-stability or drag parameters. Figure 11 indicates a 10-percent rearward shift in aerodynamic center with increasing Mach number through the transonic speed range, as would be expected for configurations of this type.

Examination of figures 6 and 7 shows that the drag polars for both the high-wing and low-wing arrangements are rotated as a result of the change in wing-section camber. Improved L/D values for the flat-bottom wing compared with either the flat-top or symmetrical wings are shown in figure 12 over the range of test lift coefficients. Figure 13 shows that the value of $(L/D)_{max}$ was between 0.7 and 1.2 greater for the flat-bottom wing than for the flat-top wing section. The effect of wing position (high wing versus low wing) was less pronounced, and within experimental accuracies no effect is shown. Similar trends and conclusions with regard to both wing section and wing position were indicated for $M = 4.63$ in reference 2. Figure 14 shows that the lift coefficient for $(L/D)_{max}$ did not shift when the wing section was changed. This result is attributed to the fact that the wing thickness was small (only 2 percent).

Figures 15 and 16 generally show insignificant effects on the lateral-directional-stability parameters, attributable to either wing section or wing-fuselage arrangement. Positive directional stability is shown at both $\alpha = 0^{\circ}$ and $10^{\circ}$; only slight deterioration occurred with angle-of-attack increases. The effective-dihedral parameter for the low-wing arrangement, however, changed sign with increasing angle of attack, and hence would cause $C_{l_\beta}/C_{n_\beta}$ to become zero for some flight conditions. Spiral instability would be expected to occur, therefore.

## CONCLUDING REMARKS

An investigation has been made of a preliminary configuration for a first-stage horizontal-take-off-and-horizontal-landing recoverable booster. Several $70^{\circ}$ delta-wing planforms with wedge-slab sections were

tested in both high-wing and low-wing arrangements with a semicylindrical fuselage in the Langley 8-foot transonic pressure tunnel to determine the longitudinal and lateral stability characteristics. The Mach numbers varied from 0.6 to 1.2 and the angle of attack ranged from $-2^{\circ}$ to $14^{\circ}$. Data were obtained at both $0^{\circ}$ and $5^{\circ}$ of sideslip. Reynolds numbers per foot for the tests varied from $1.6 \times 10^{6}$ to $4.2 \times 10^{6}$.

The results showed that approximately equal increments in pitching moment resulted from progressively changing the wing section from a flat-bottom to a symmetrical section, and finally to a flat-top section. Negative pitching-moment increments also resulted from changing from the high-wing to the low-wing arrangement. Longitudinal stability was generally unaffected by either wing section or wing-fuselage arrangement. Increases in lift-drag ratio, up to 1.2, resulted from changing from the flat-top to the flat-bottom wing, but the lift-drag ratio was about the same for the high-wing and low-wing arrangements. Changes in either wing section or wing position did not significantly alter the lateral-directional stability characteristics.

Langley Research Center,
National Aeronautics and Space Administration,
Langley Station, Hampton, Va., March 22, 1962.

## REFERENCES

1. Pierpont, P. Kenneth: Transonic Stability of a Preliminary Vertical-Take-Off Launch Configuration With a Horizontal-Landing Recoverable Booster. NASA TM X-689, 1962.

2. Robins, A. Warner, Reed, James D., and Harris, Roy V., Jr.: Effects of Wing Section and Body Vertical Location on the Longitudinal Aerodynamic Characteristics at Mach Number 4.63 of a Configuration Having a $70^{\circ}$ Delta Wing and a Low Volume Body. NASA TM X-552, 1961.

3. Braslow, Albert L., and Knox, Eugene C.: Simplified Method for Determination of Critical Height of Distributed Roughness Particles for Boundary-Layer Transition at Mach Numbers From 0 to 5. NACA TN 4363, 1958.

L
1
9
7
5

TABLE I.- GEOMETRIC CHARACTERISTICS OF MODEL

| | |
|---|---|
| Length, overall, in. | 33.00 |
| Fuselage: | |
| Length, in. | 33.00 |
| Diameter, in. | 2.52 |
| Forebody fineness ratio, Length/Diameter | 7.0 |
| Afterbody fineness ratio, Length/Diameter | 6.1 |
| Base area, sq in. | 4.16 |
| Wing: | |
| Total area, sq in. | 396 |
| Span, in. | 24.00 |
| Root chord, in. | 33.00 |
| Tip chord, in. | 0.00 |
| Leading-edge sweep, deg | 70 |
| Mean aerodynamic chord, in. | 22.00 |
| Moment reference center, percent $\bar{c}$ | 25 |
| Moment reference center, in. from base | 16.50 |
| Vertical tail: | |
| Area (exposed), sq in. | 16.43 |
| Span, in. | 3.46 |
| Root chord, in. | 9.50 |
| Tip chord, in. | 0.00 |
| Leading-edge sweep, deg | 70 |

Design forebody coordinates

| x | Radius | x | Radius |
|---|---|---|---|
| 0 | 0 | 11.720 | 1.116 |
| .720 | .101 | 12.720 | 1.160 |
| 1.720 | .234 | 13.720 | 1.196 |
| 2.720 | .358 | 14.720 | 1.224 |
| 3.720 | .475 | 15.720 | 1.244 |
| 4.720 | .583 | 16.720 | 1.256 |
| 5.720 | .684 | 17.720 | 1.260 |
| 6.720 | .776 | ↓ | ↓ |
| 7.720 | .860 | | |
| 8.720 | .936 | 33.720 | 1.260 |
| 9.720 | 1.004 | | |
| 10.720 | 1.064 | | |

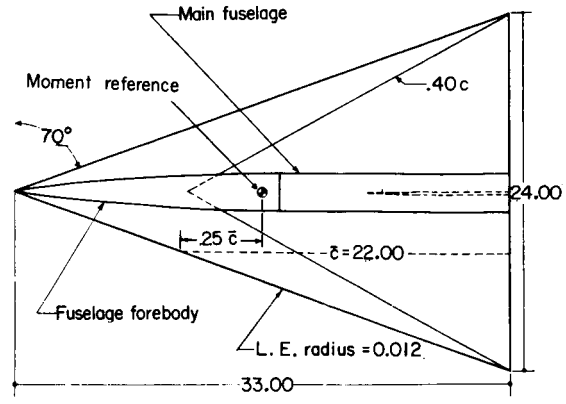


Plan view

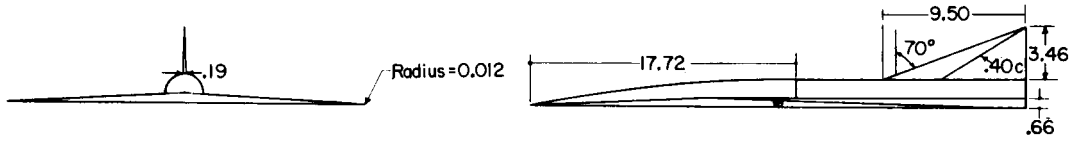


Low-wing arrangement, flat-bottom wing

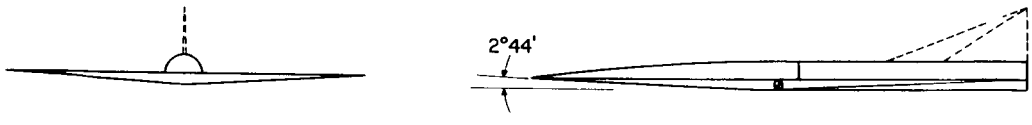


Low-wing arrangement, flat-top wing

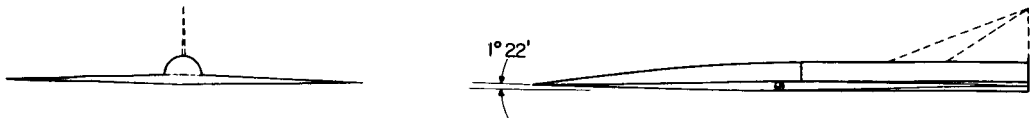


Low-wing arrangement, symmetrical wing

Figure 1.- General arrangement of model. All linear dimensions are in inches.

L-1975

L-1975

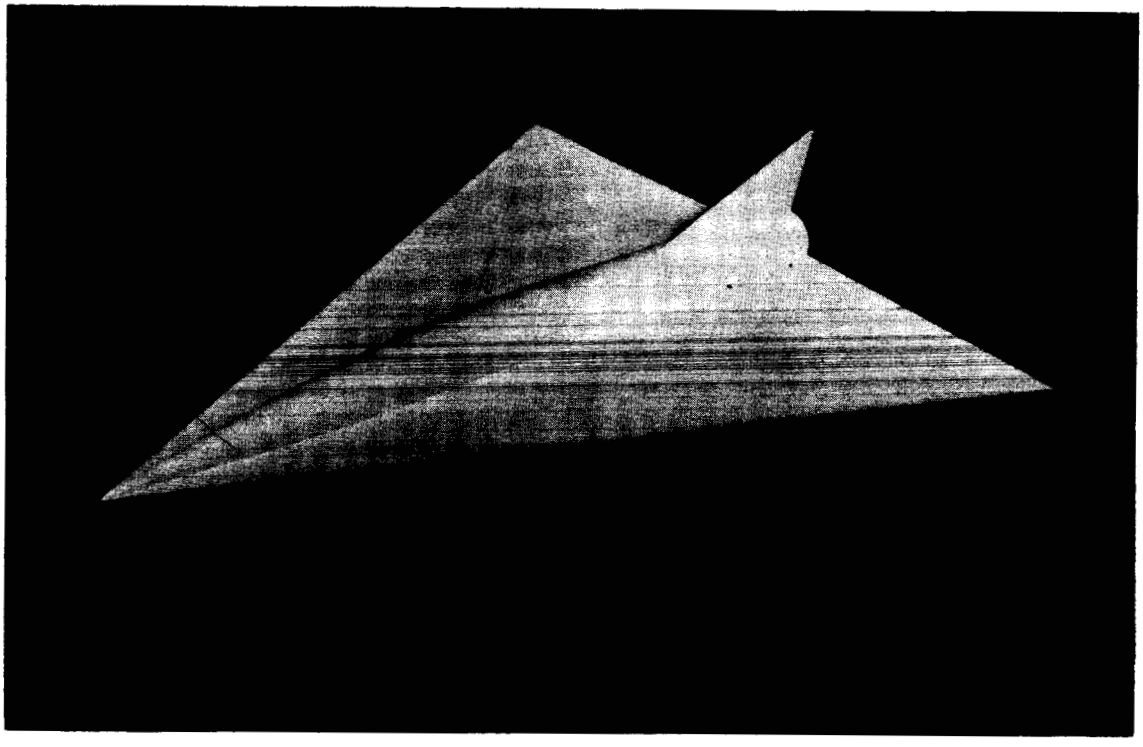

(a) Three-quarter front view. L-61-2668

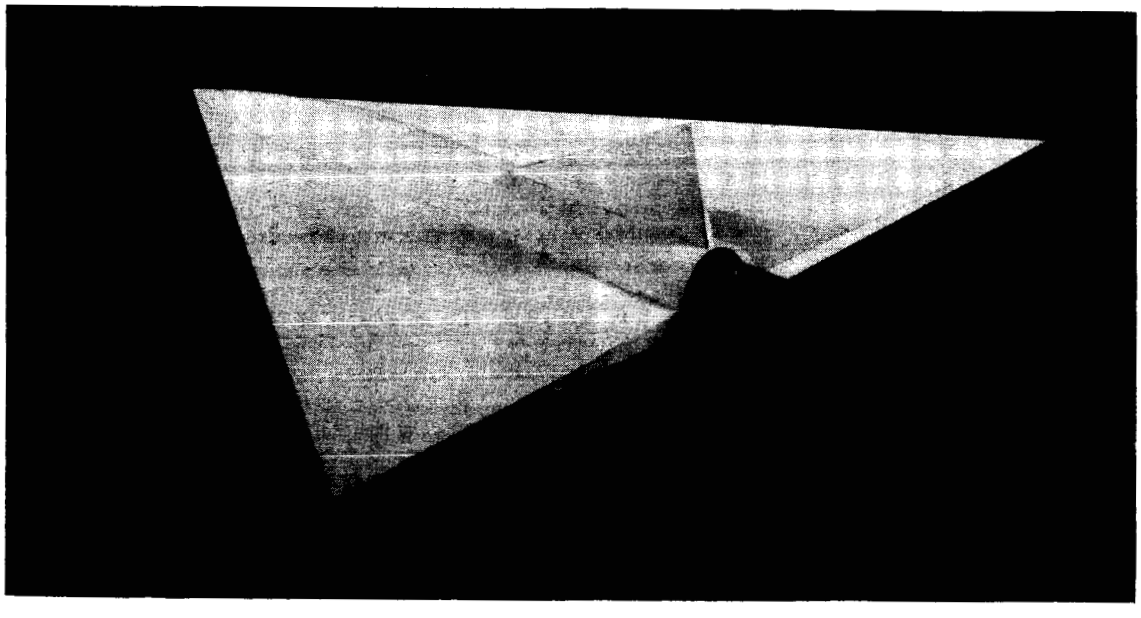

(b) Three-quarter rear view. L-61-2669

Figure 2.- Photographs of low-wing recoverable booster with symmetrical wing installed.

UNCLASSIFIED
~~CONFIDENTIAL~~

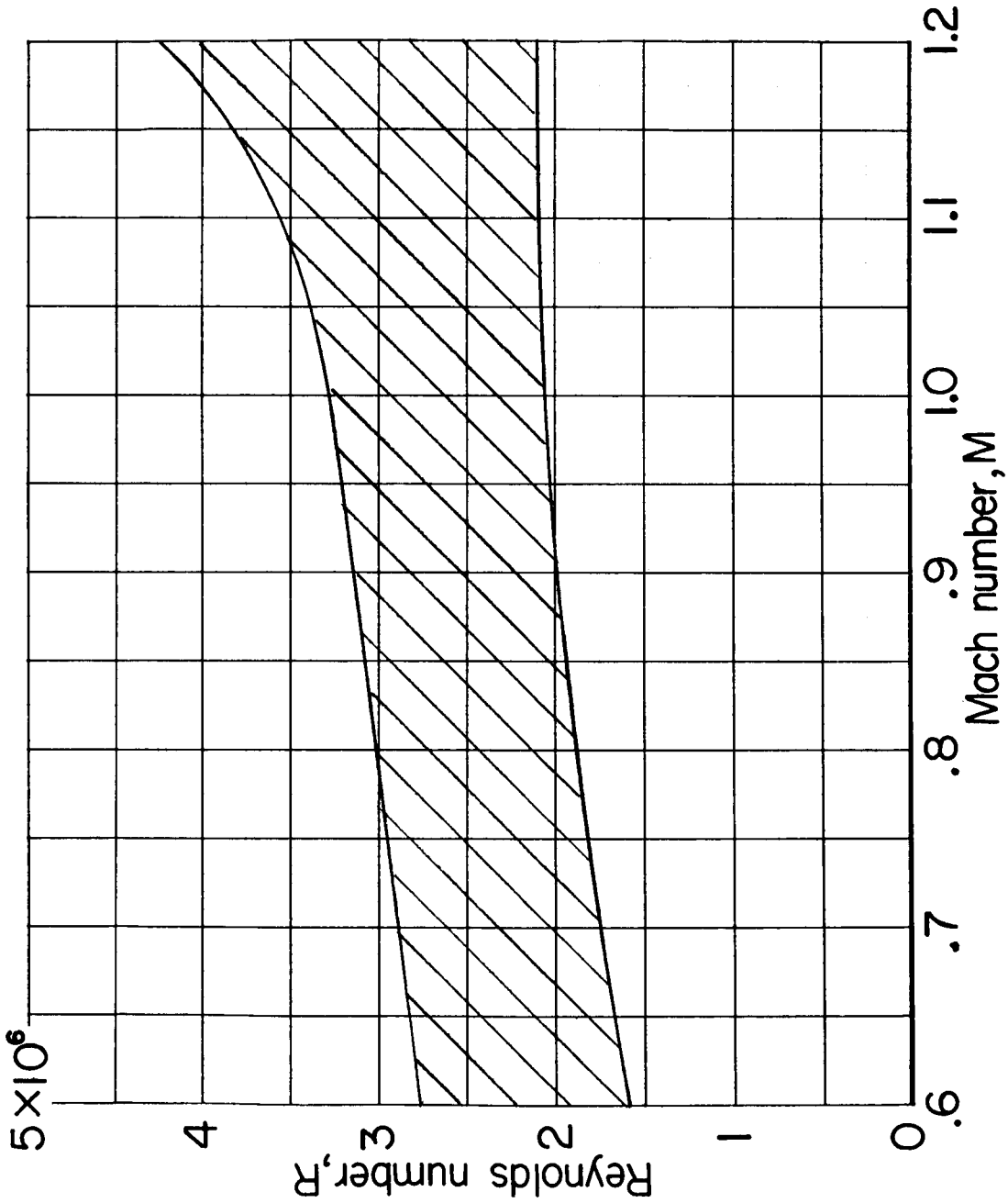


Figure 3.- Variation with Mach number of test Reynolds number per foot.

L-1975

~~CONFIDENTIAL~~
UNCLASSIFIED

L-1975

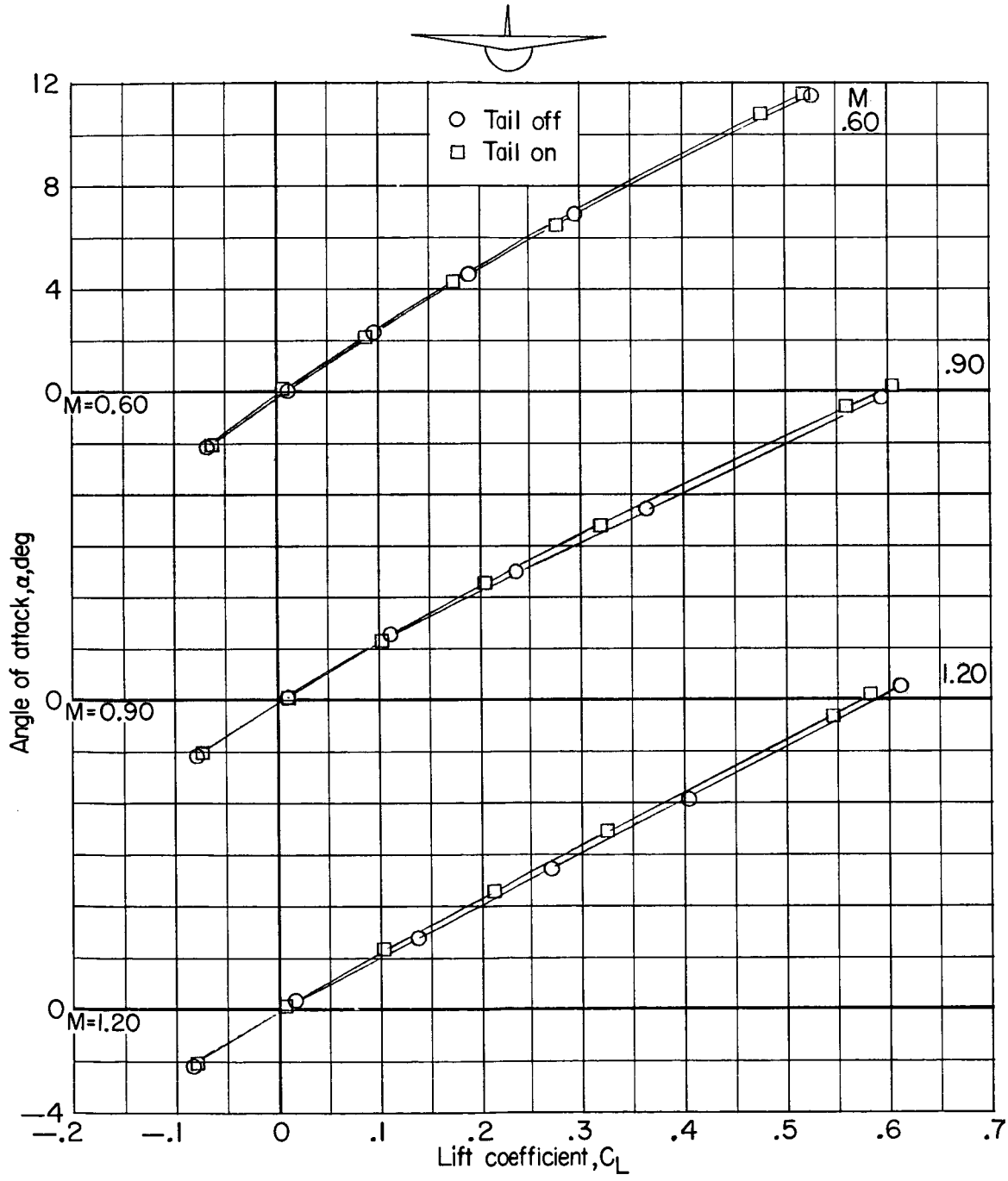


(a) Angle of attack plotted against lift coefficient.

Figure 4.- Aerodynamic characteristics of the high-wing arrangement with the flat-top wing without and with vertical tail. $\beta = 0^{\circ}$.

UNCLASSIFIED
[redacted]

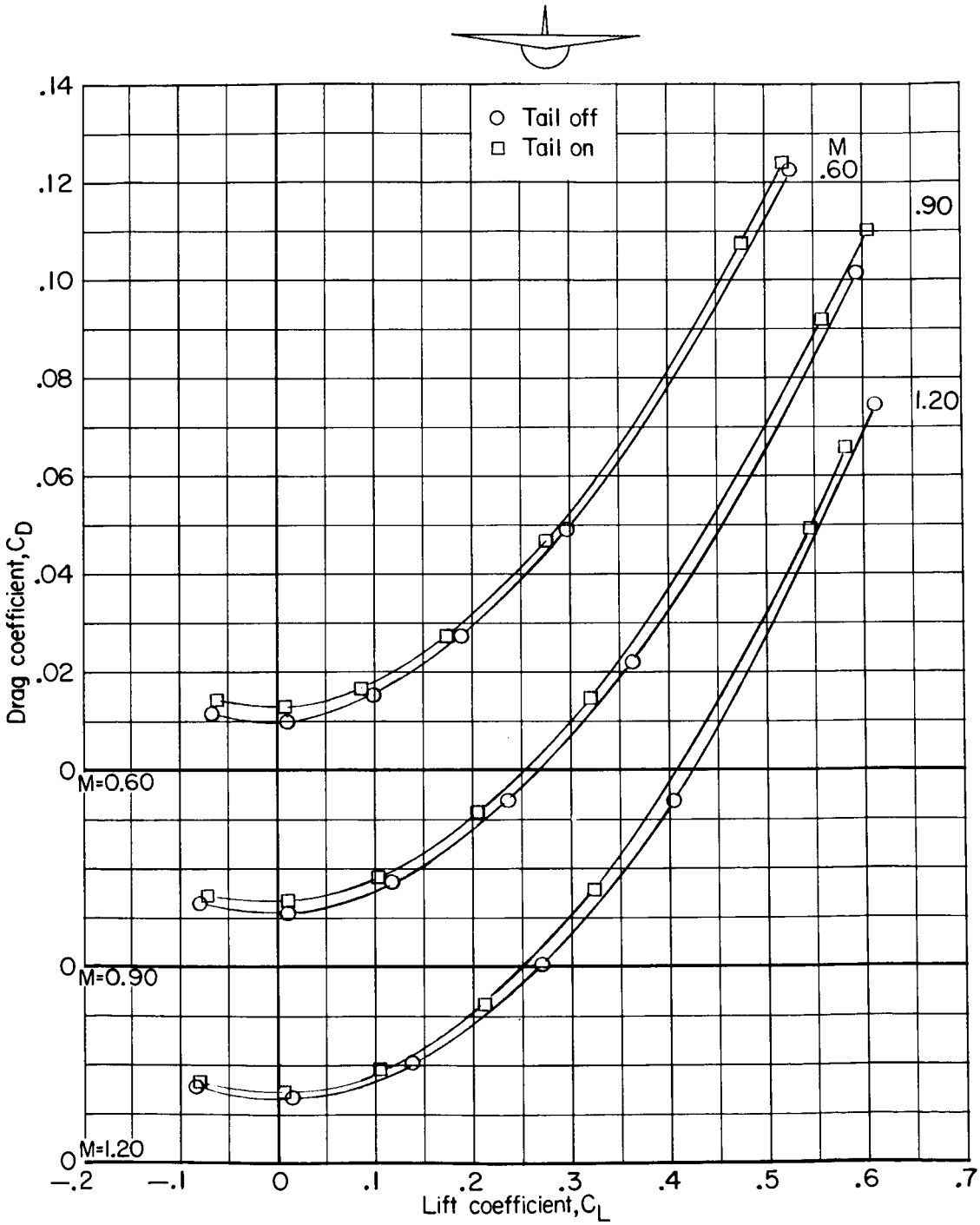


(b) Drag coefficient plotted against lift coefficient.

Figure 4.- Continued.

[redacted]
UNCLASSIFIED

L-1975

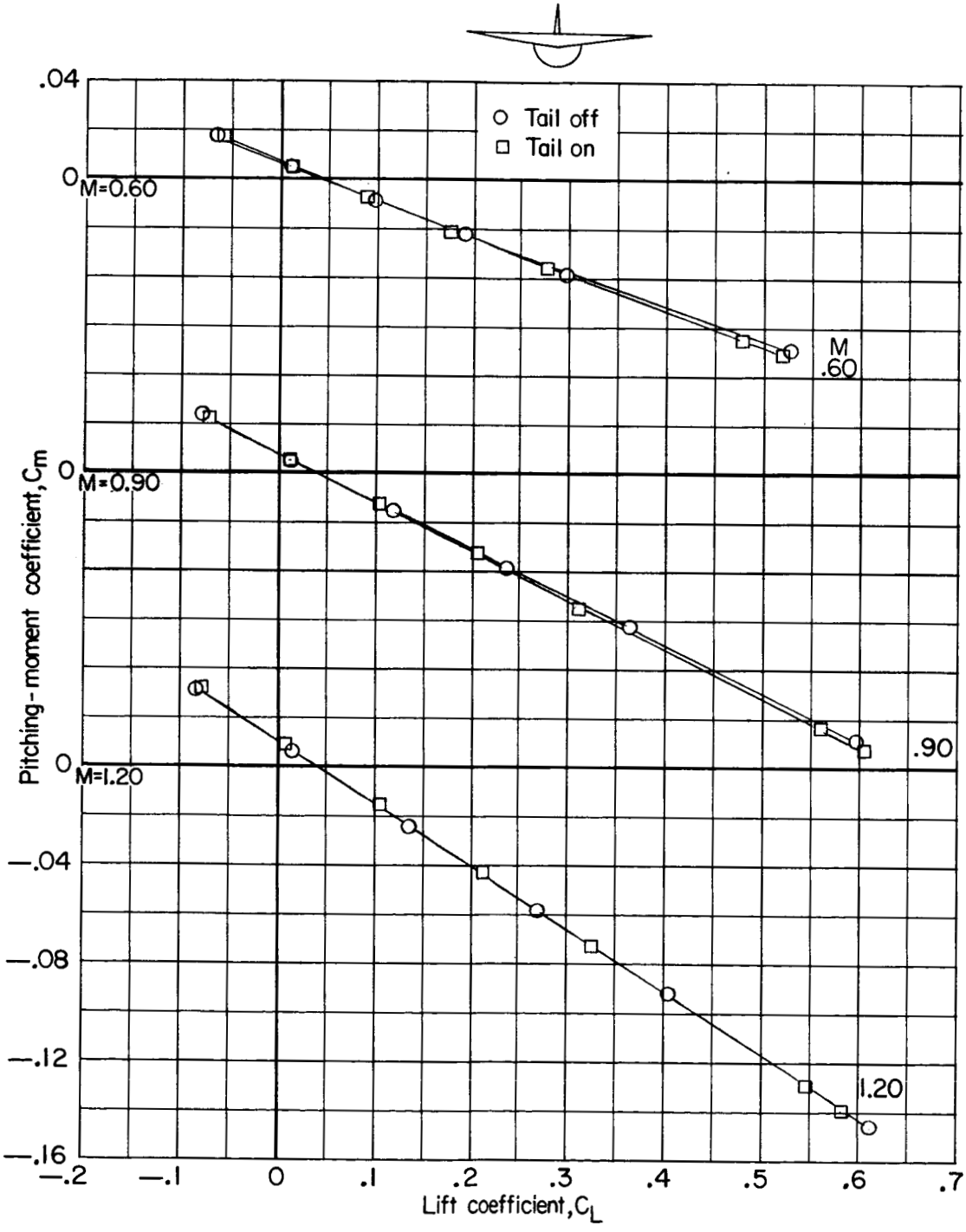


(c) Pitching-moment coefficient plotted against lift coefficient.

Figure 4.- Continued.

UNCLASSIFIED
[redacted]

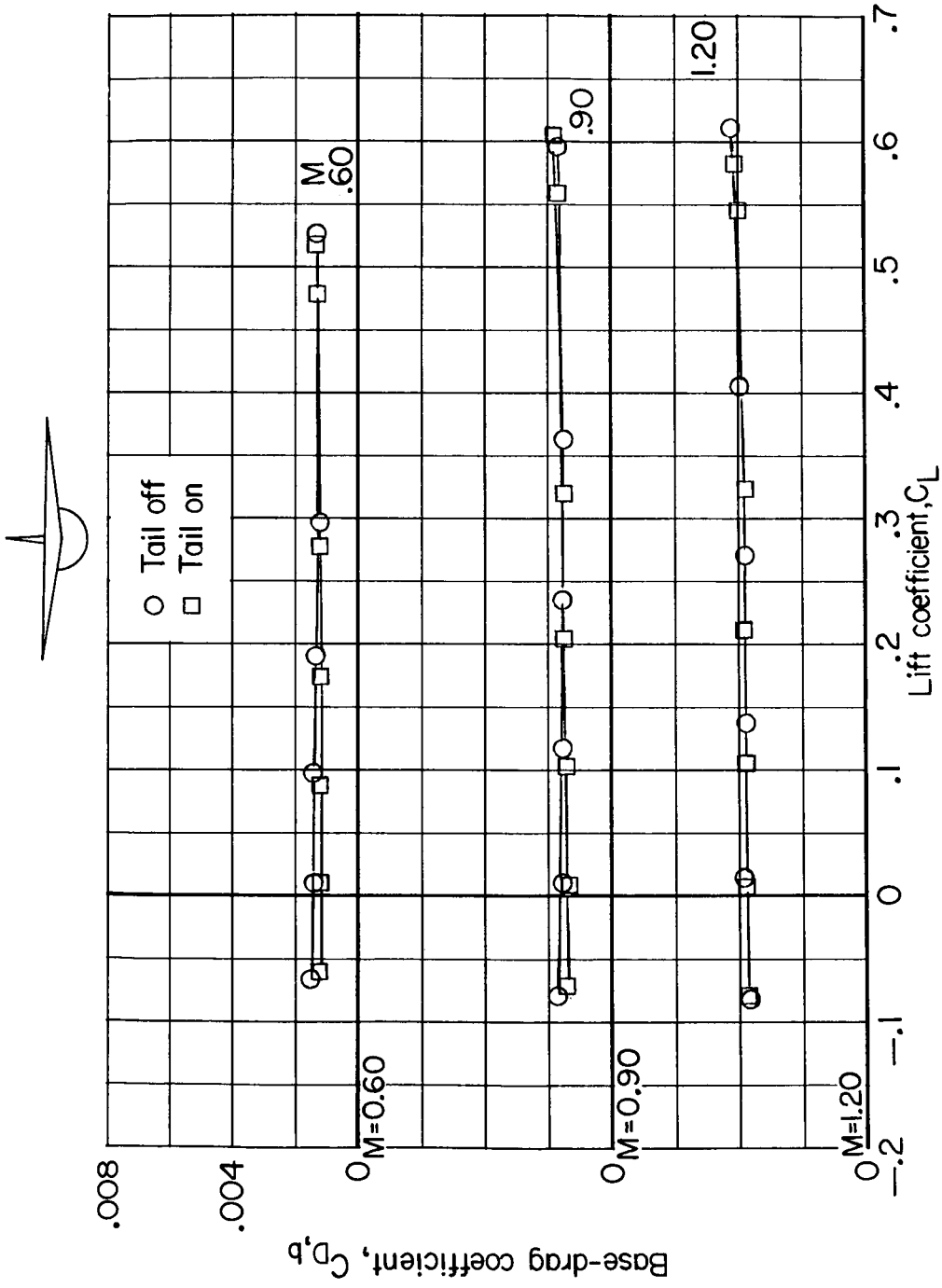


(d) Base-drag coefficient plotted against lift coefficient.

Figure 4.- Concluded.

L-1075

[redacted]
UNCLASSIFIED

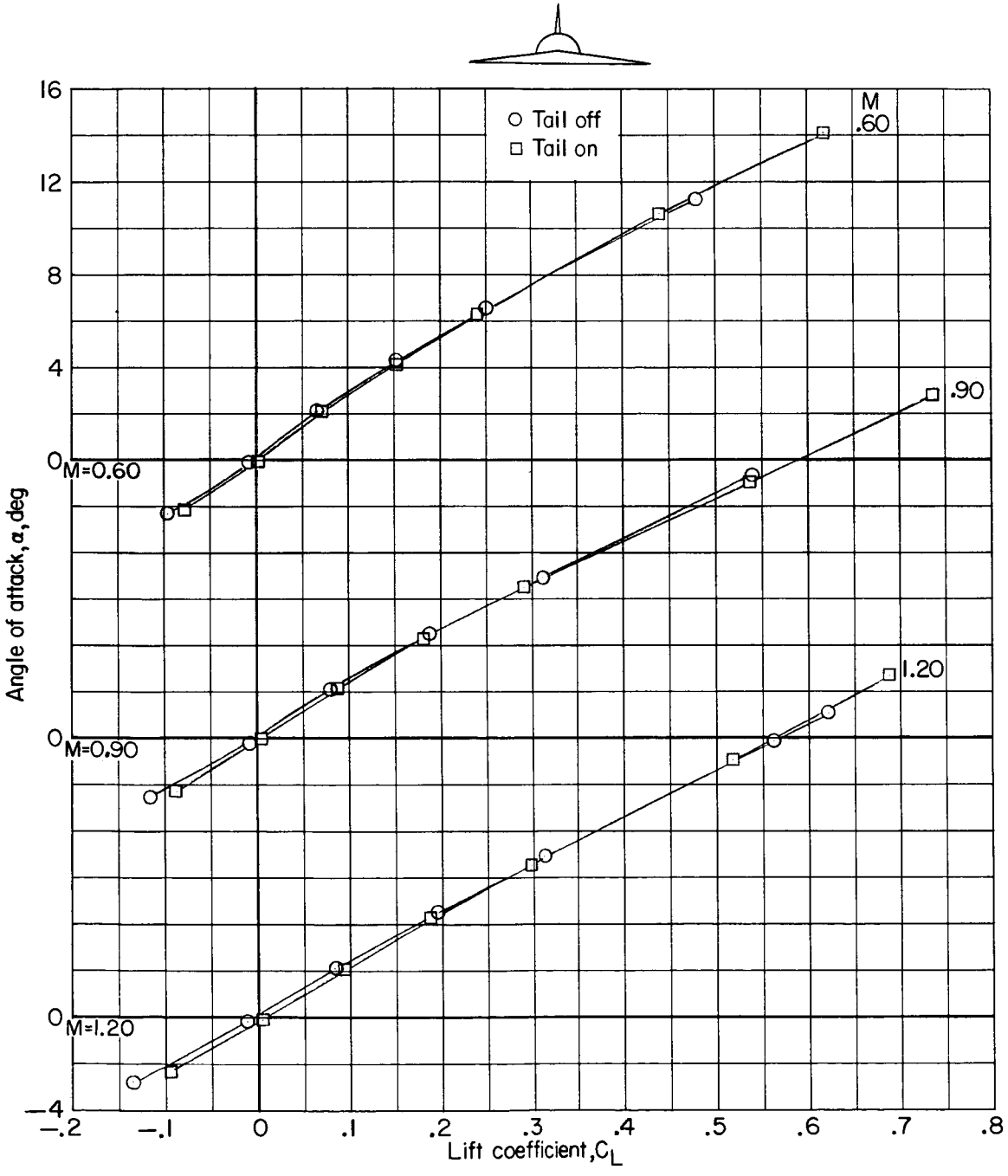


(a) Angle of attack plotted against lift coefficient.

Figure 5.- Aerodynamic characteristics of the low-wing arrangement with the flat-bottom wing without and with vertical tail. $\beta = 0^{\circ}$.

UNCLASSIFIED



[redacted]

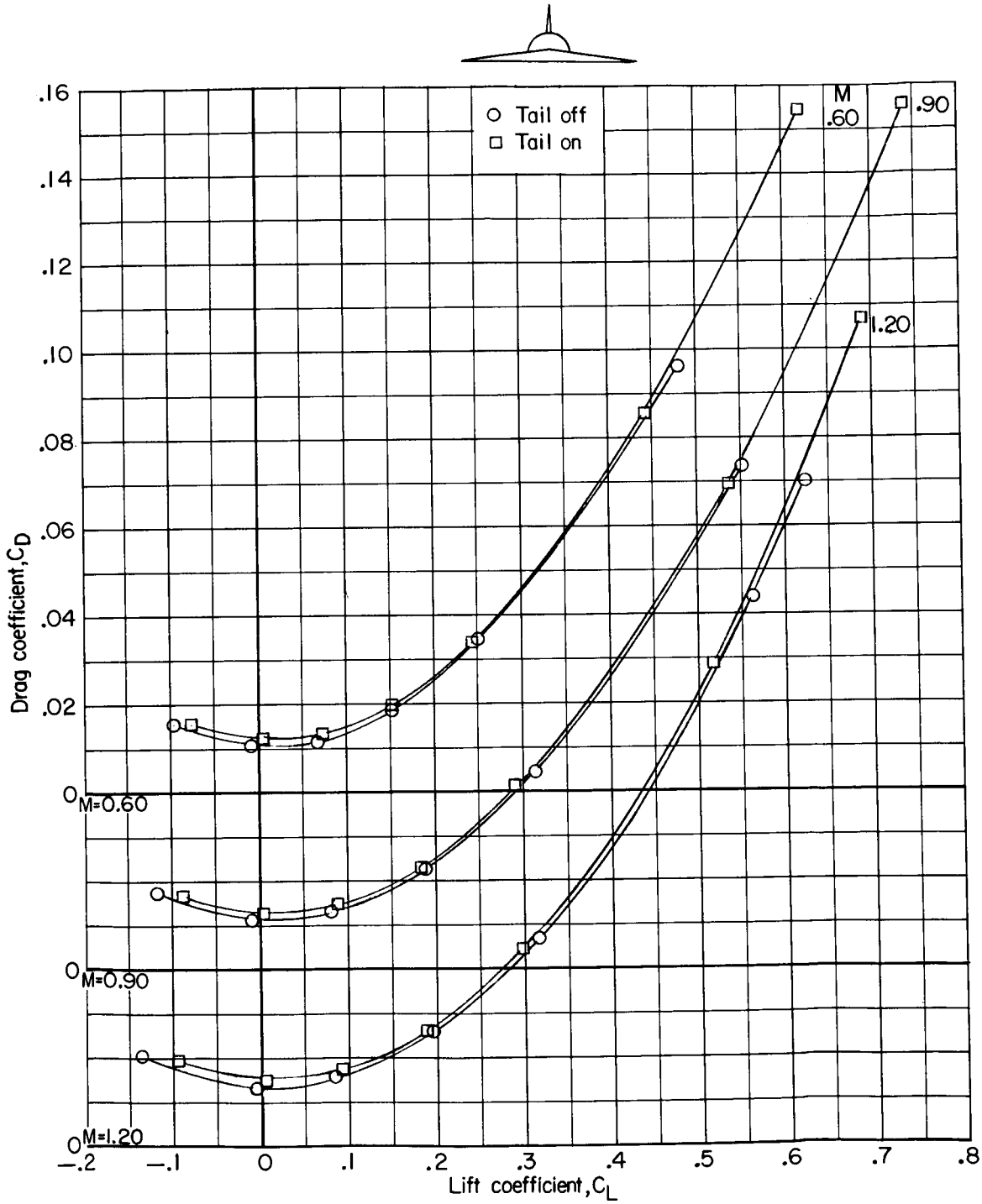


(b) Drag coefficient plotted against lift coefficient.

Figure 5.- Continued.

[redacted]
UNCLASSIFIED

L-1975

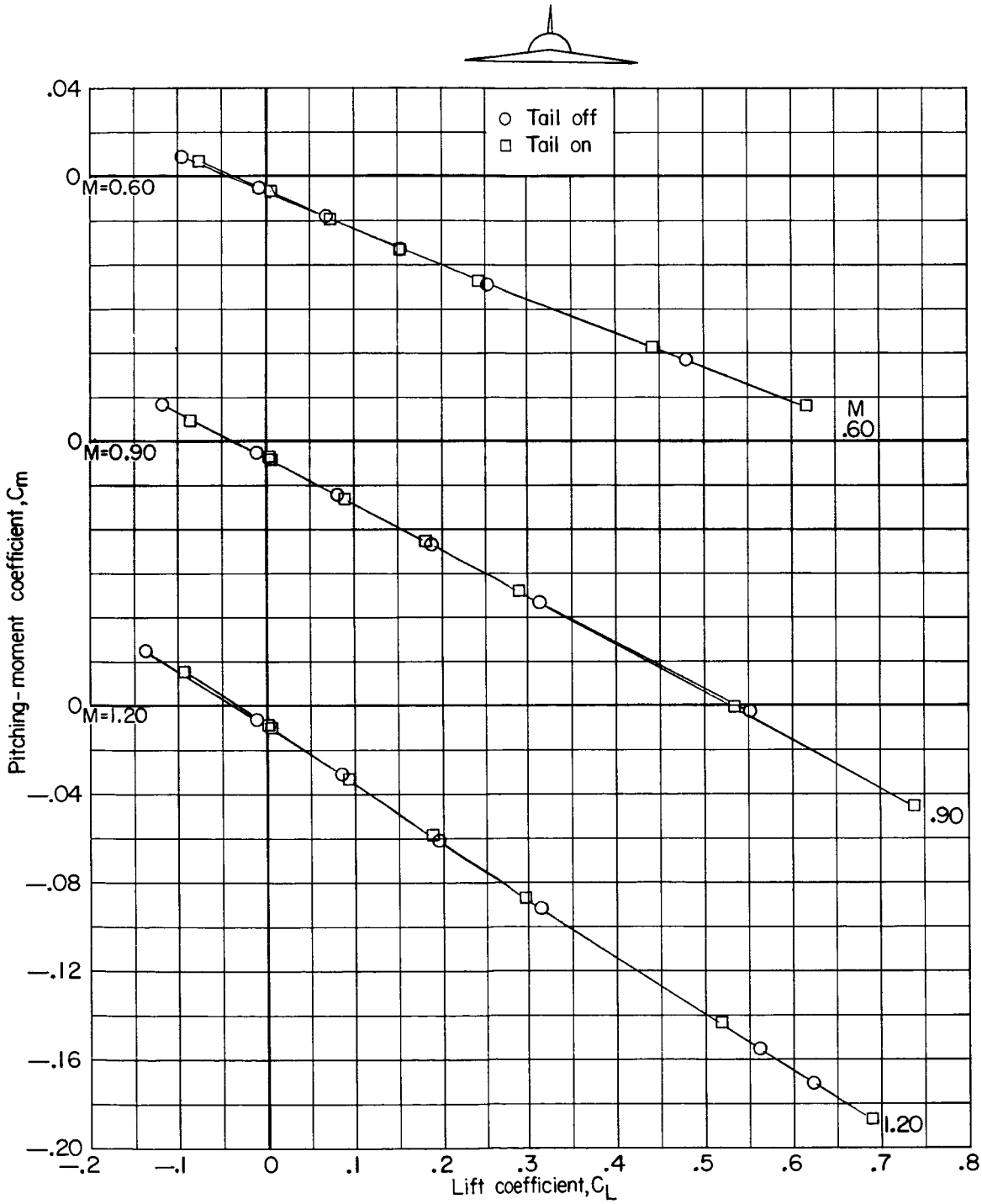


(c) Pitching-moment coefficient plotted against lift coefficient.

Figure 5.- Continued.

UNCLASSIFIED
CONFIDENTIAL

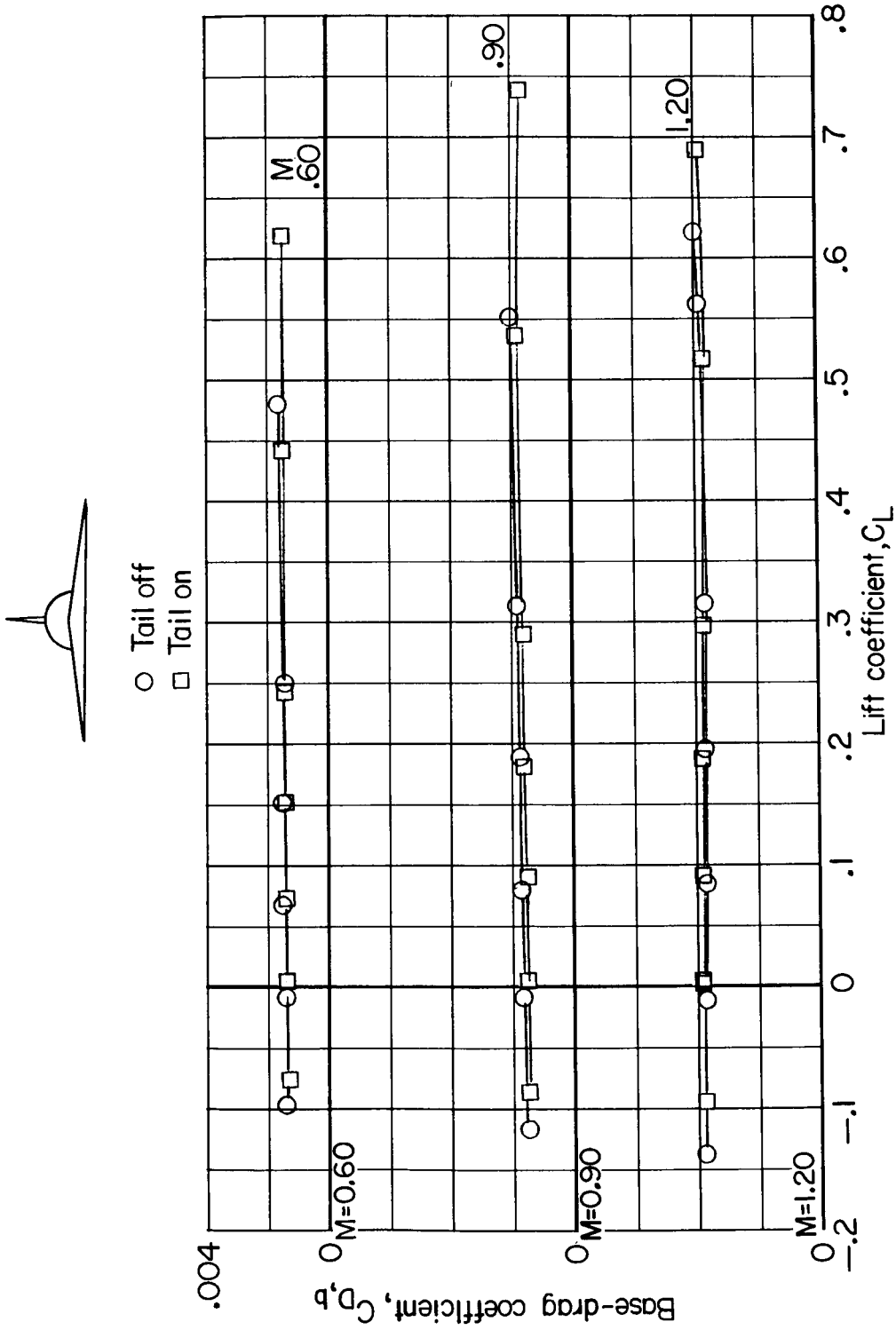


(d) Base-drag coefficient plotted against lift coefficient.

Figure 5.- Concluded.

UNCLASSIFIED
CONFIDENTIAL

L-1975

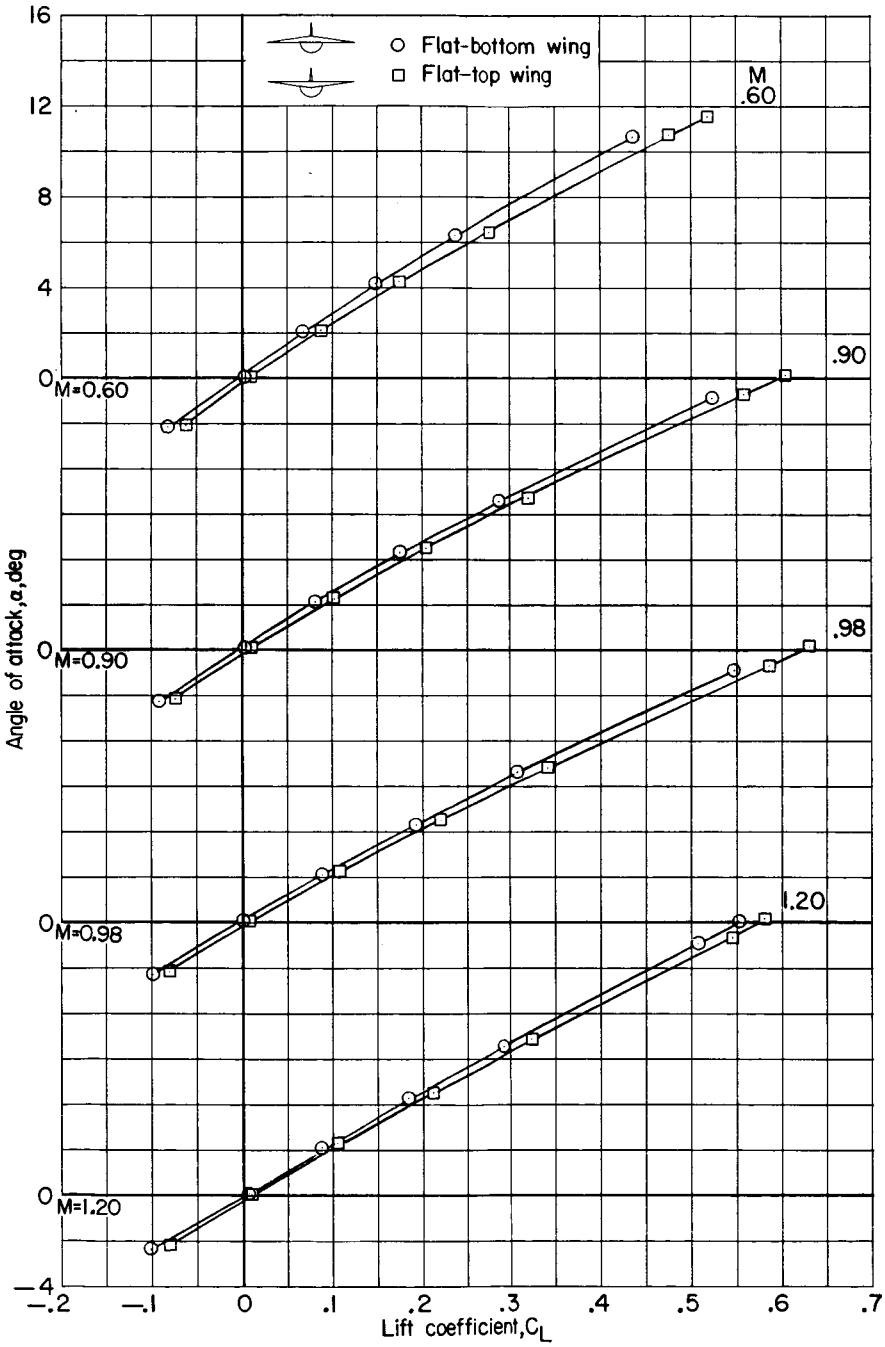


(a) Angle of attack plotted against lift coefficient.

Figure 6.- Effect of wing section on the aerodynamic characteristics of the high-wing arrangement. $\beta = 0^{\circ}$.

UNCLASSIFIED

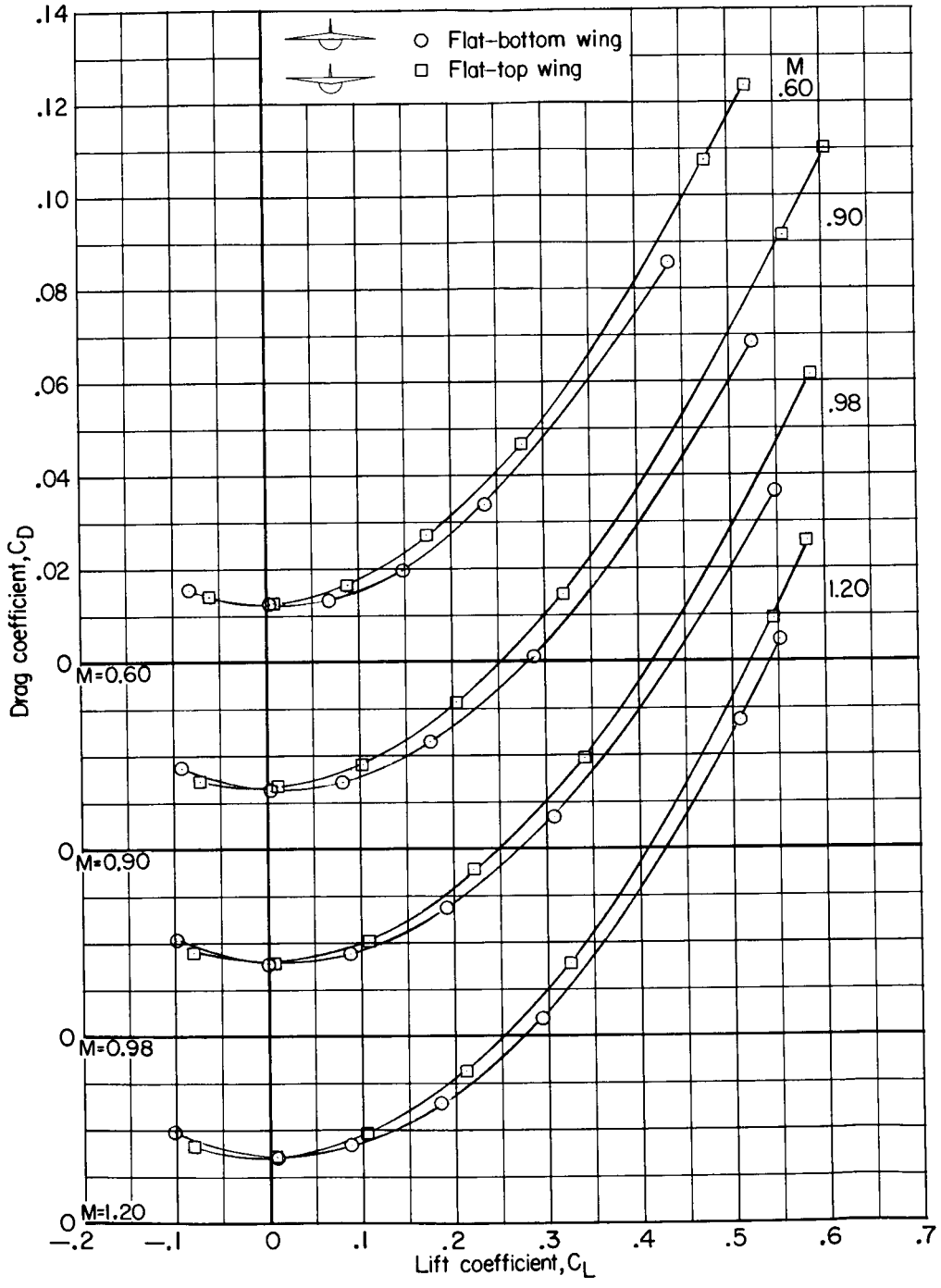


(b) Drag coefficient plotted against lift coefficient.

Figure 6.- Continued.

~~CONFIDENTIAL~~ UNCLASSIFIED

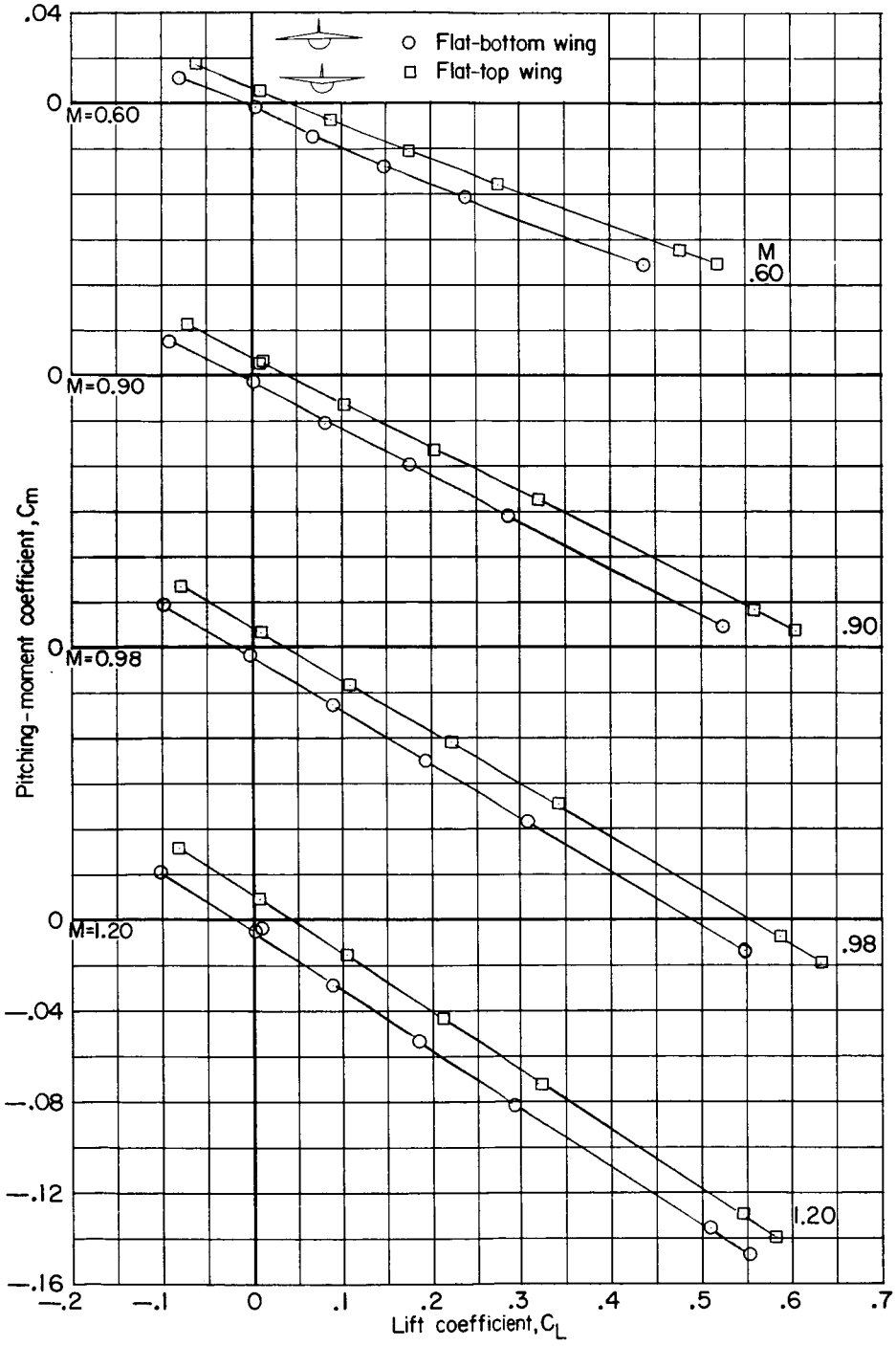


(c) Pitching-moment coefficient plotted against lift coefficient.

Figure 6.- Continued.

UNCLASSIFIED [redacted]

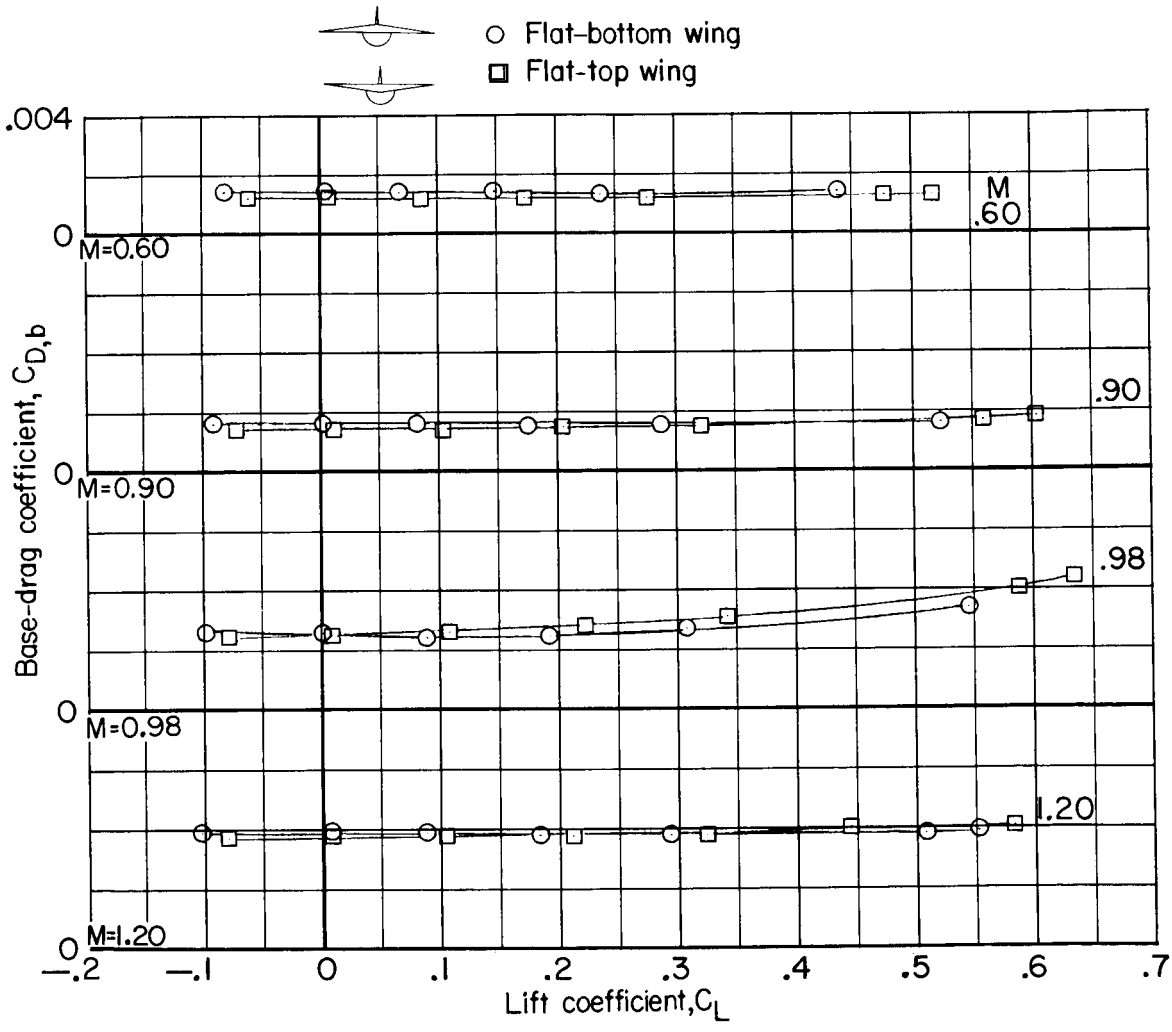


(d) Base-drag coefficient plotted against lift coefficient.

Figure 6.- Concluded.

[redacted]
UNCLASSIFIED

L-1975

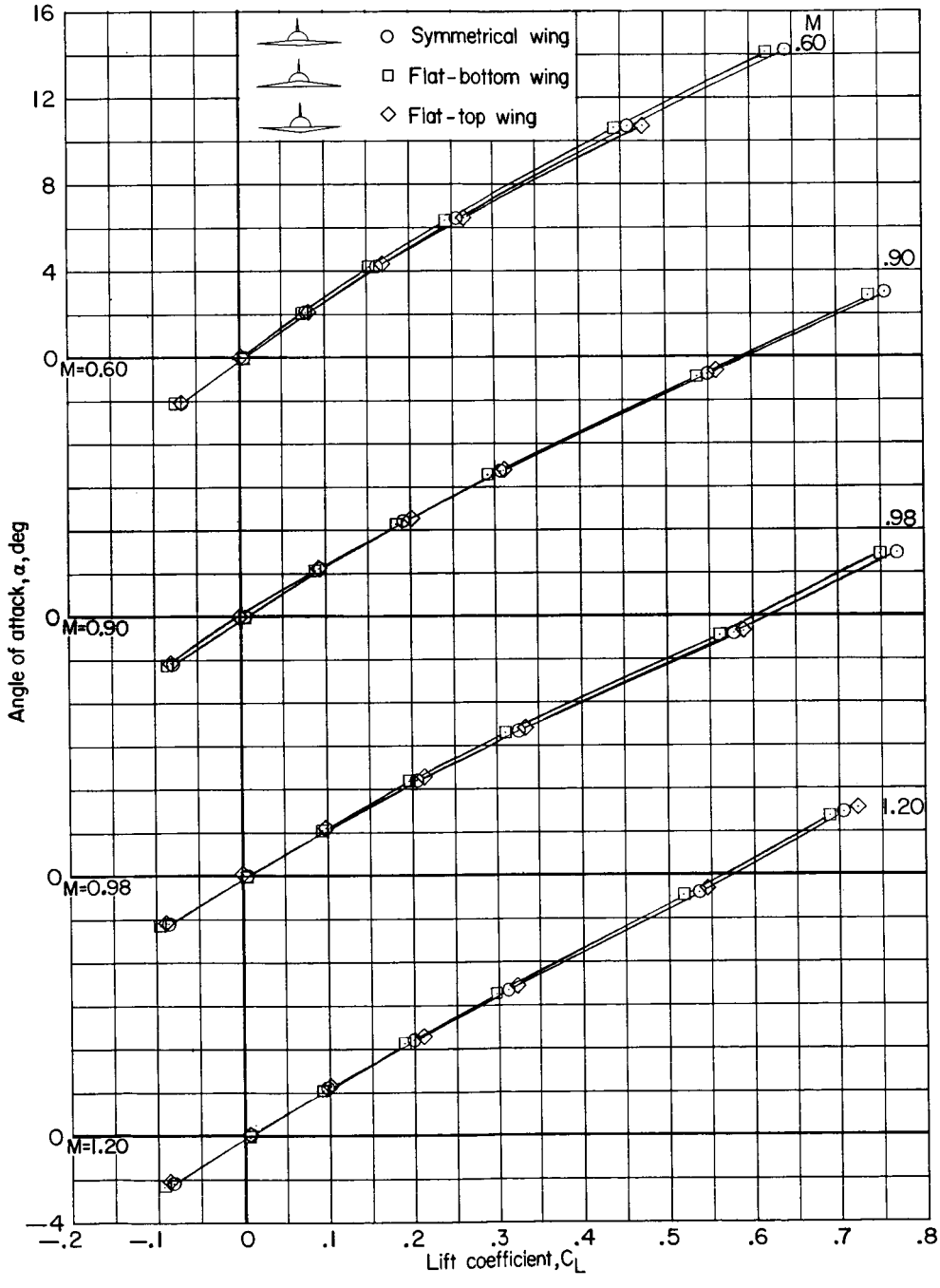


(a) Angle of attack plotted against lift coefficient.

Figure 7.- Effect of wing section on the aerodynamic characteristics of the low-wing arrangement. $\beta = 0^{\circ}$.

UNCLASSIFIED

[redacted]

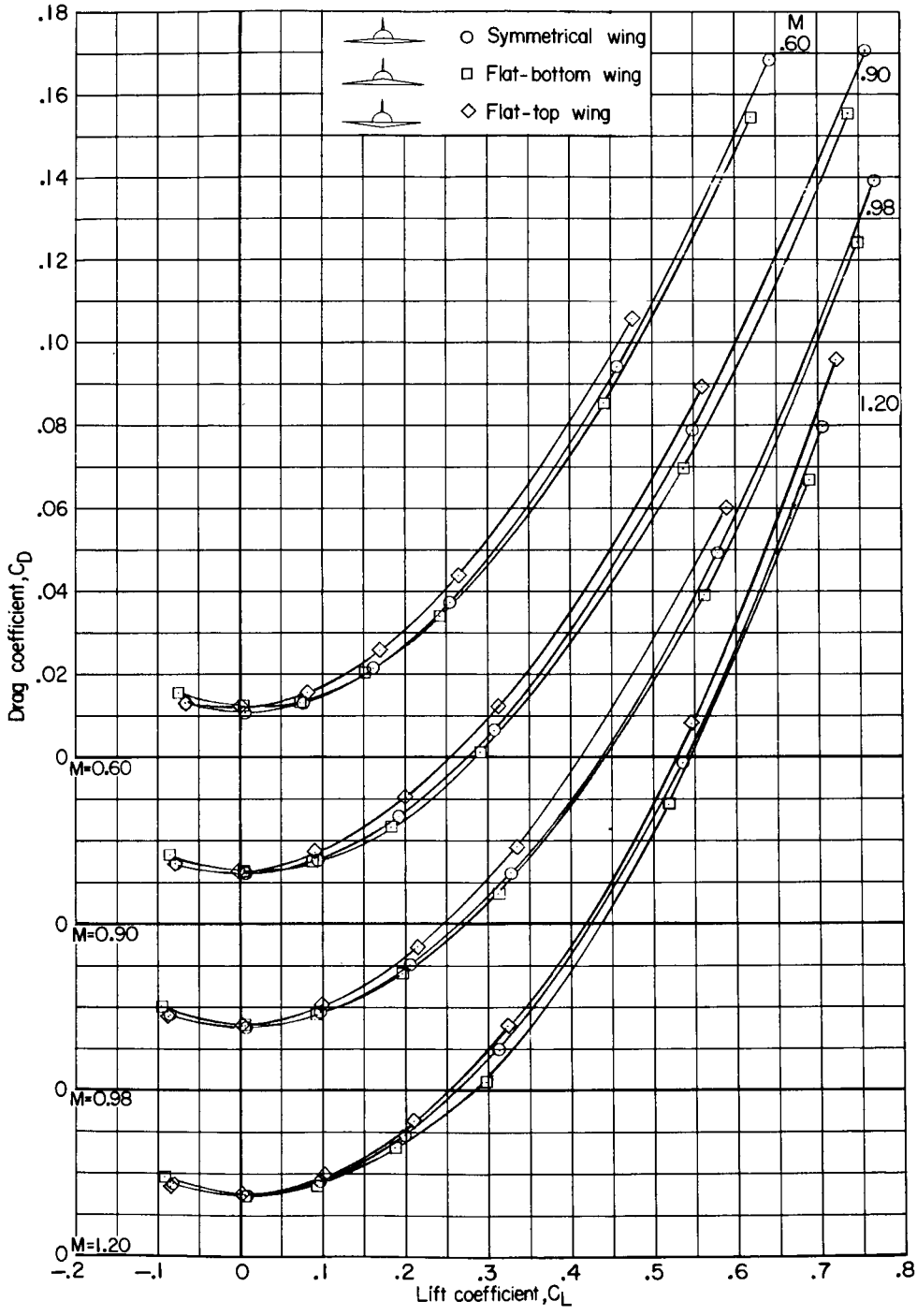


(b) Drag coefficient plotted against lift coefficient.

Figure 7.- Continued.

L-1975

[redacted]

UNCLASSIFIED

L-1975

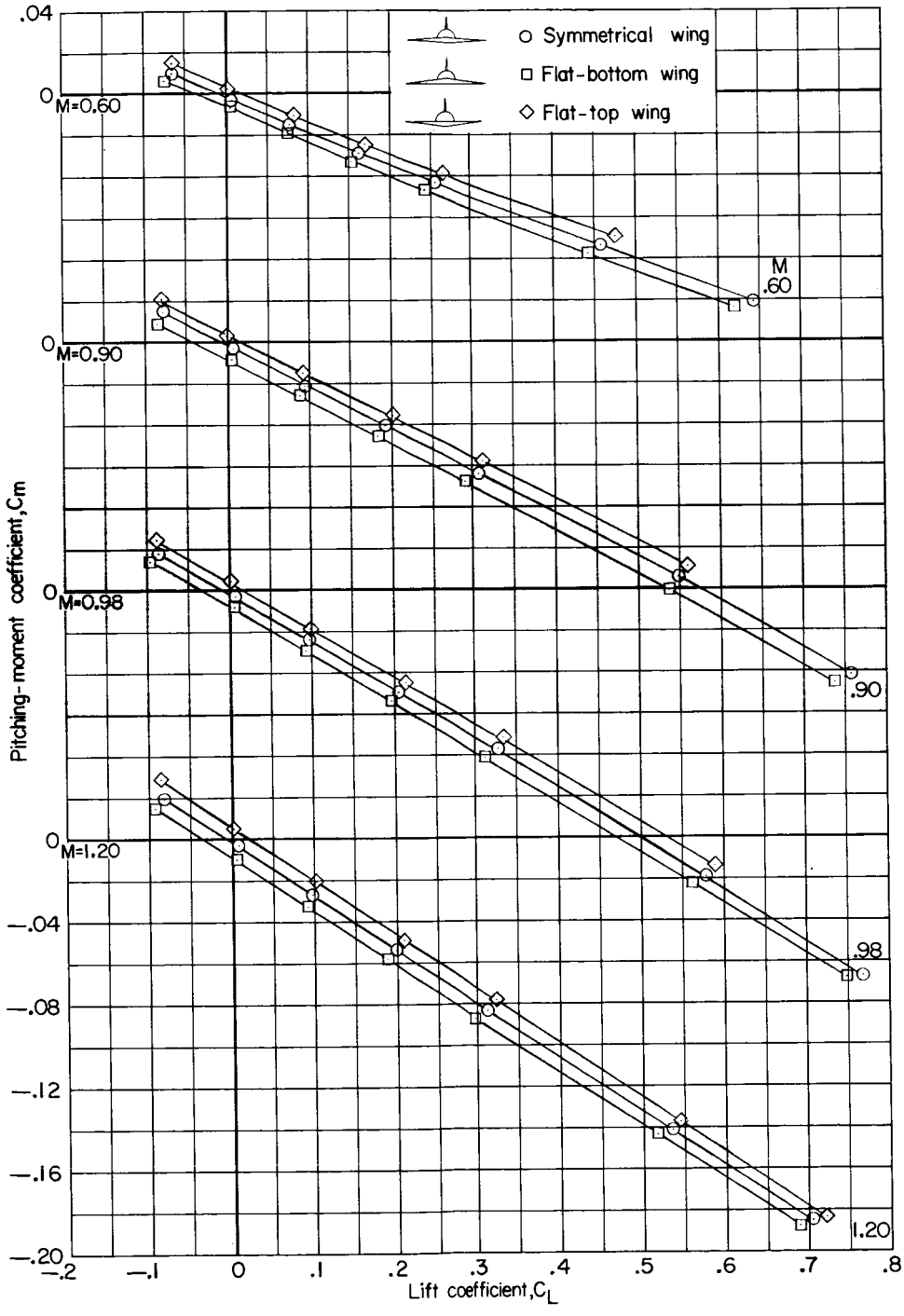


(c) Pitching-moment coefficient plotted against lift coefficient.

Figure 7.- Continued.

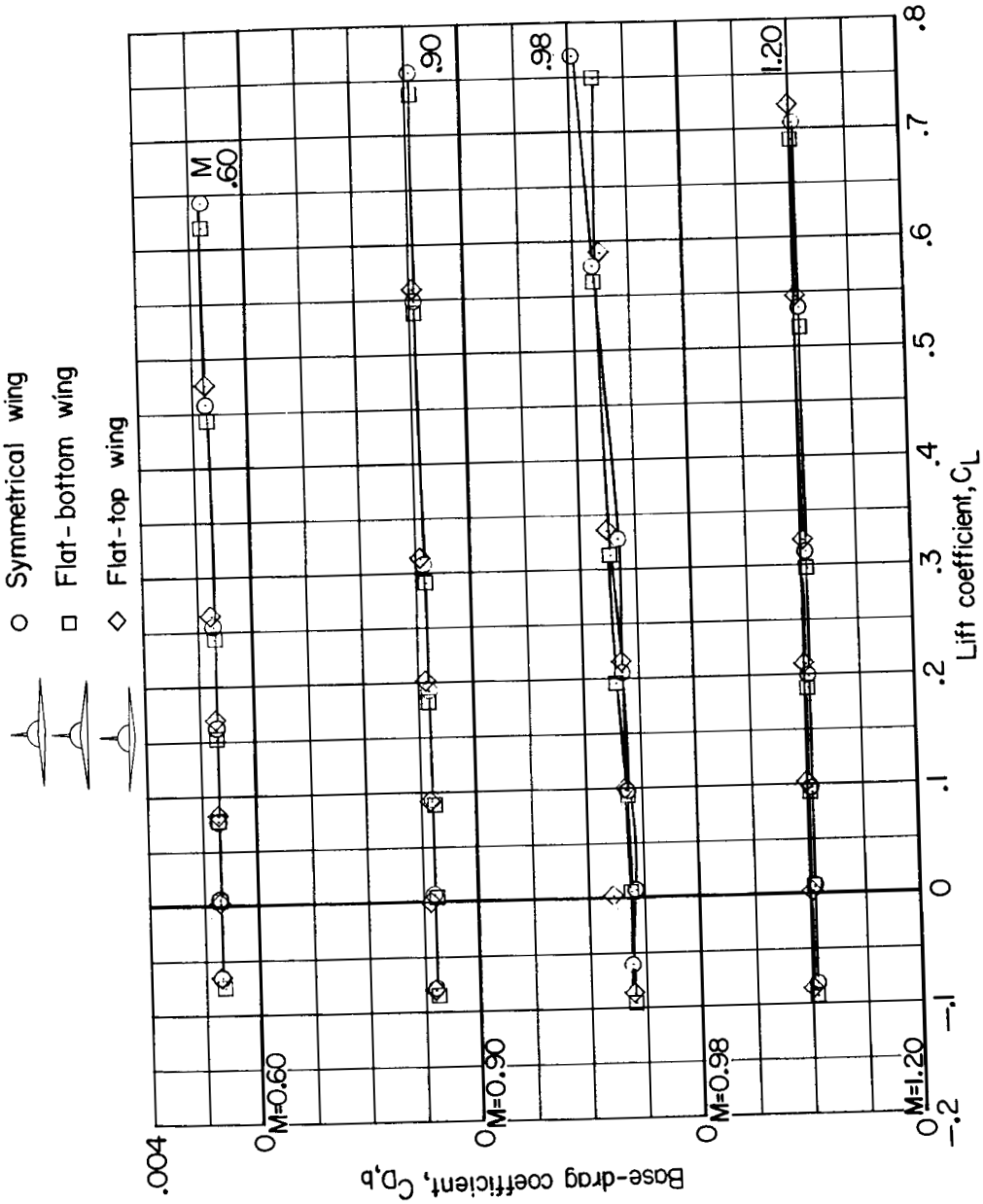


(d) Base-drag coefficient plotted against lift coefficient.

Figure 7.- Concluded.

L-1975

L-1975

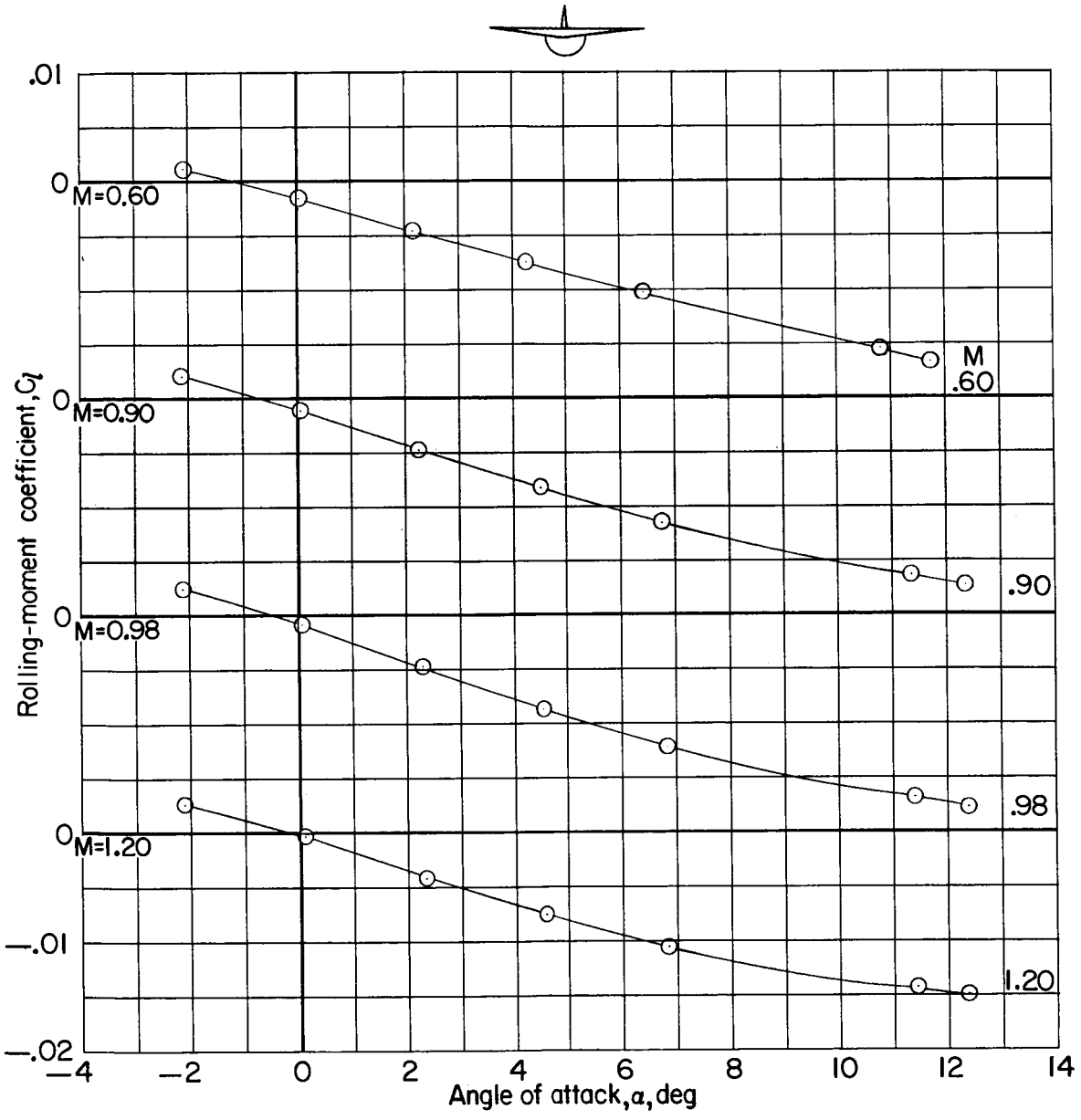


(a) Rolling-moment coefficient plotted against angle of attack.

Figure 8.- Aerodynamic characteristics of the high-wing arrangement with flat-top wing at 5° of sideslip.

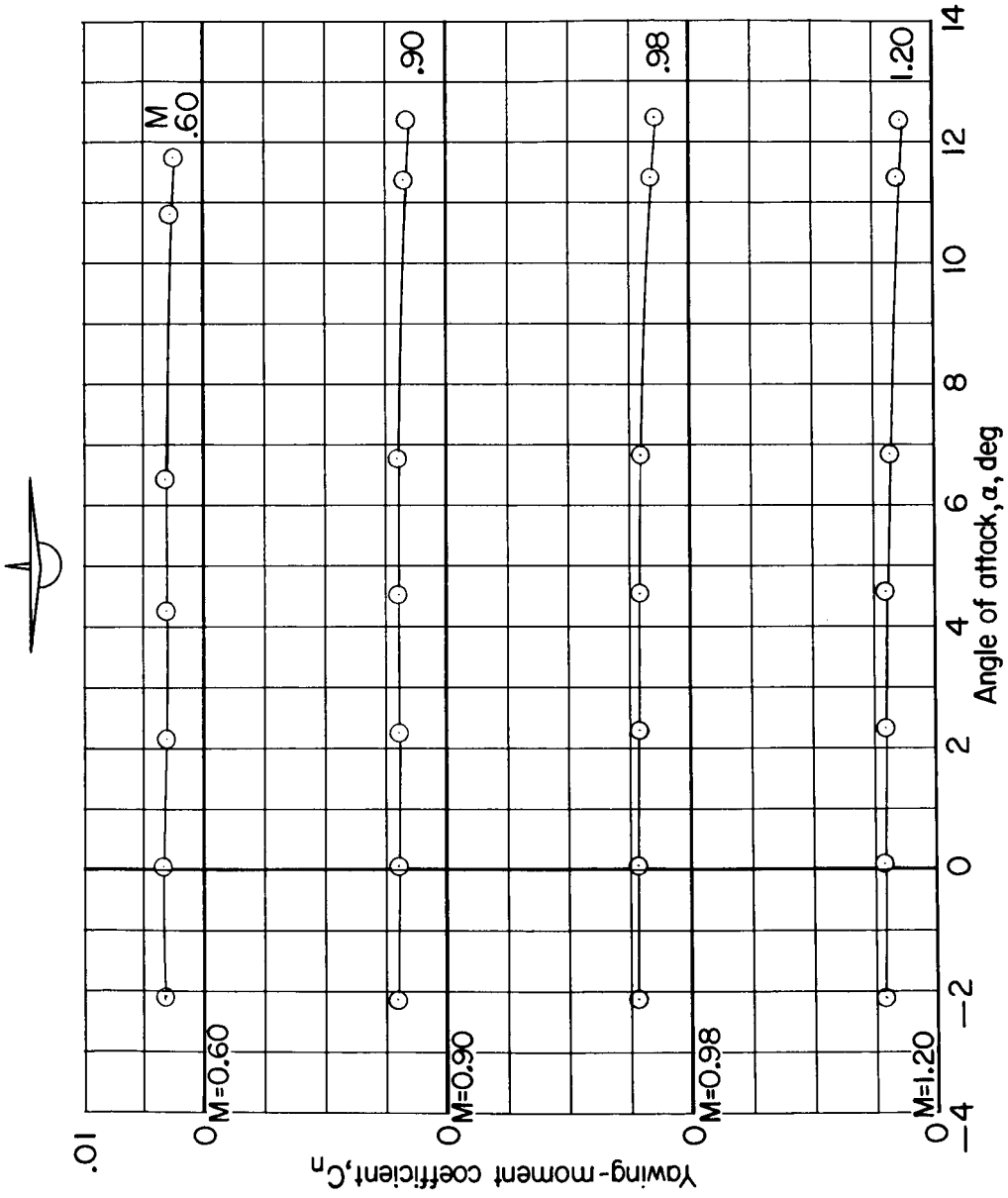


(b) Yawing-moment coefficient plotted against angle of attack.

Figure 8.- Continued.

L-1975

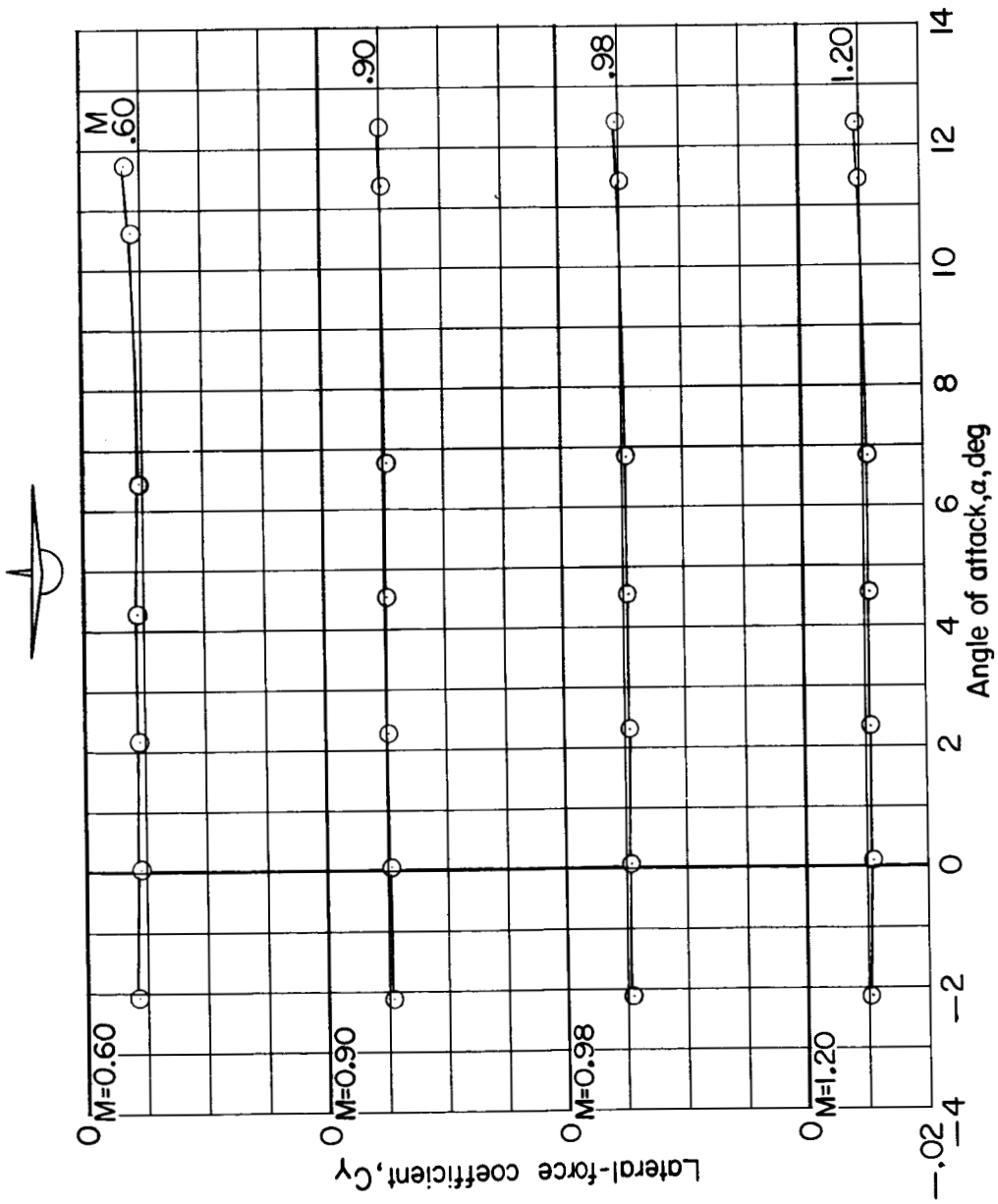


(c) Lateral-force coefficient plotted against angle of attack.

Figure 8.- Concluded.

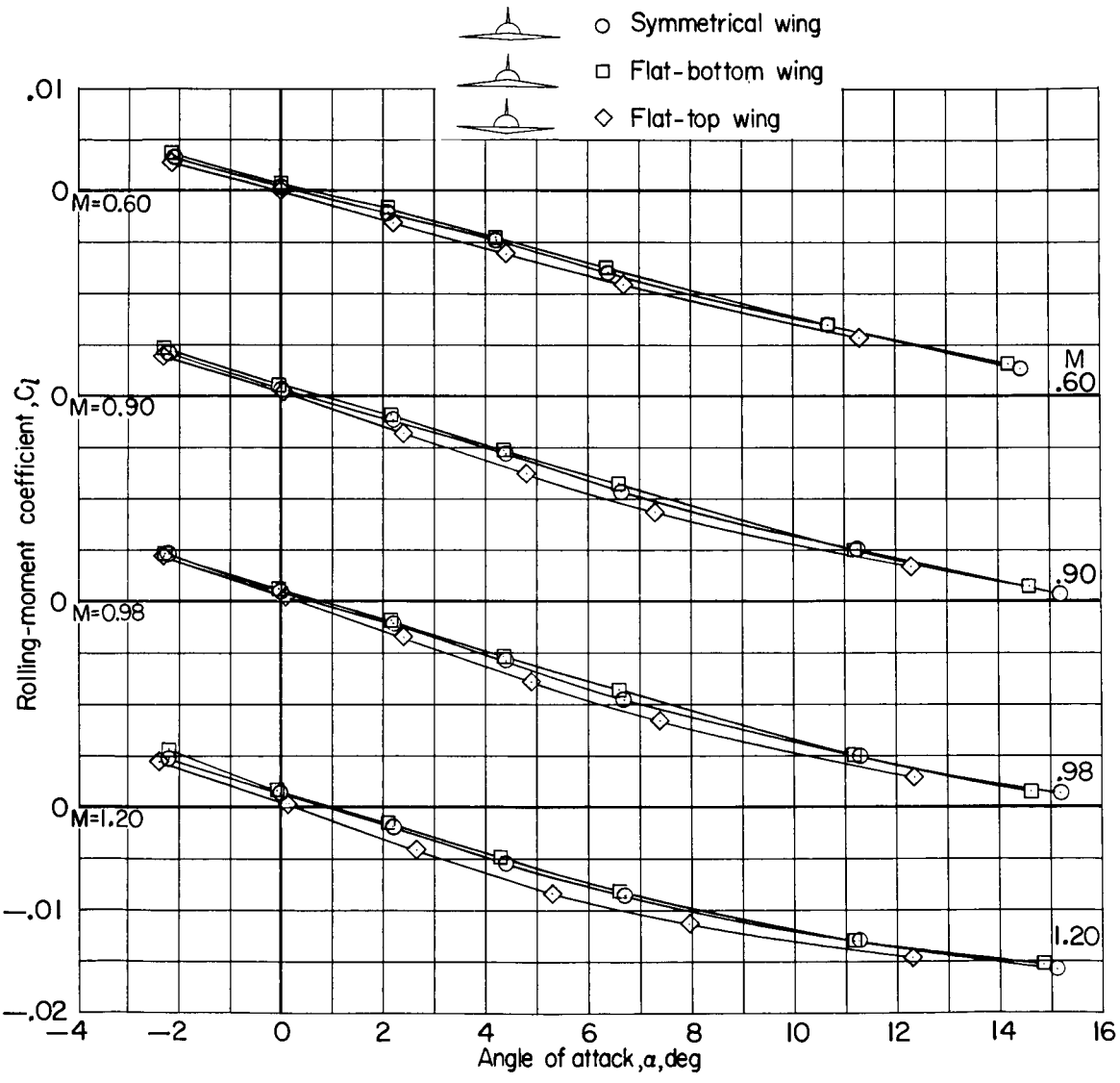


(a) Rolling-moment coefficient plotted against angle of attack.

Figure 9.- Effect of wing section on the aerodynamic characteristics of the low-wing arrangement at 5° of sideslip.

L-1975

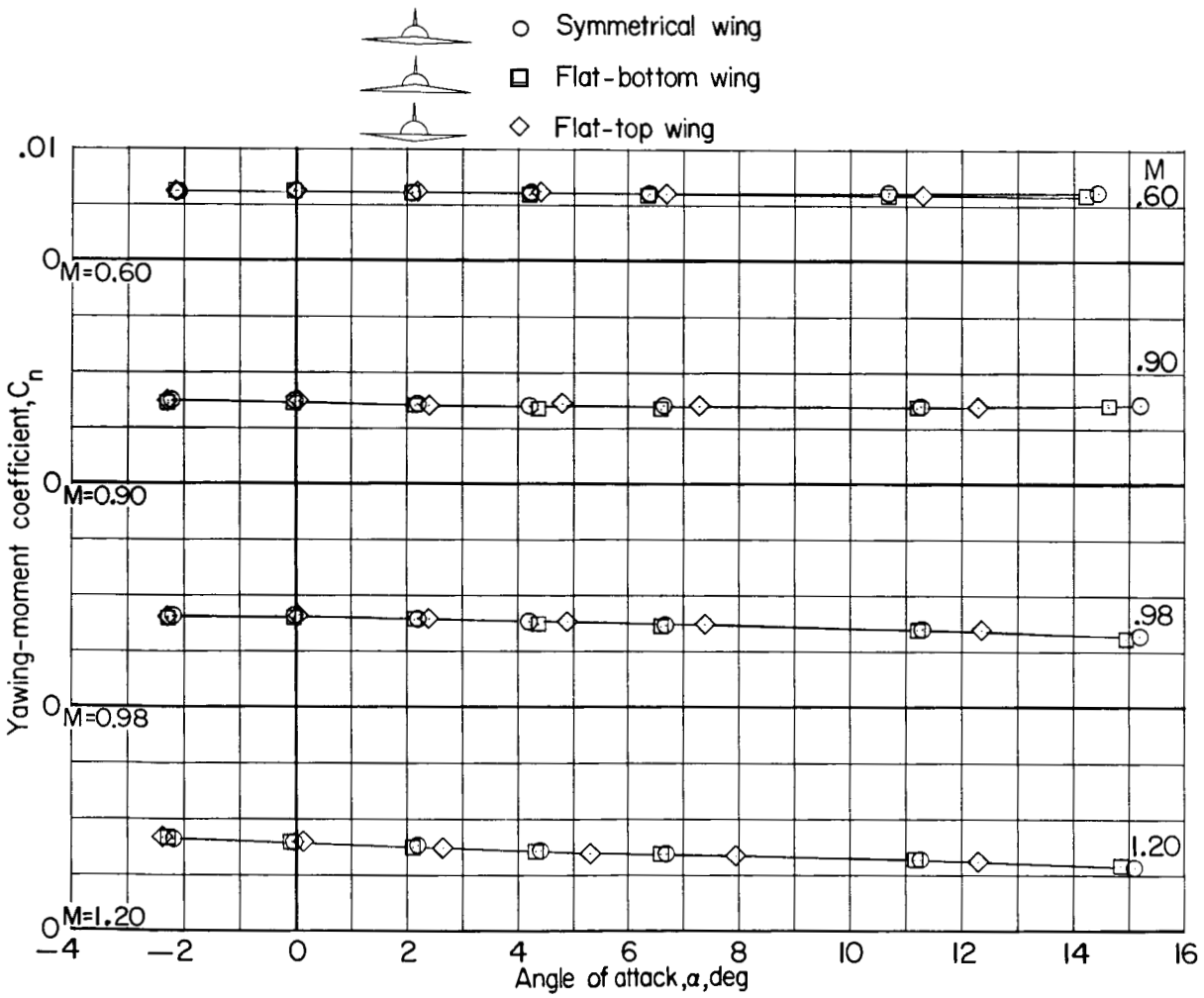


(b) Yawing-moment coefficient plotted against angle of attack.

Figure 9.- Continued.

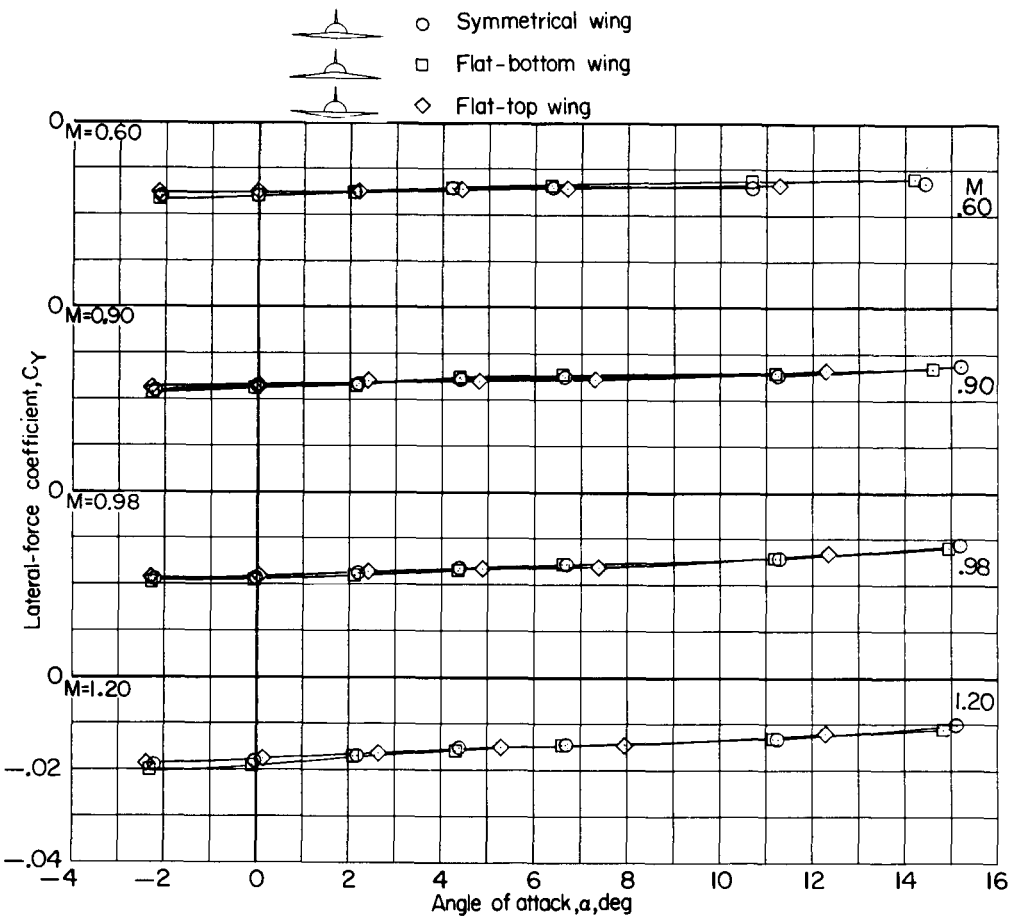


(c) Lateral-force coefficient plotted against angle of attack.

Figure 9.- Concluded.

UNCLASSIFIED

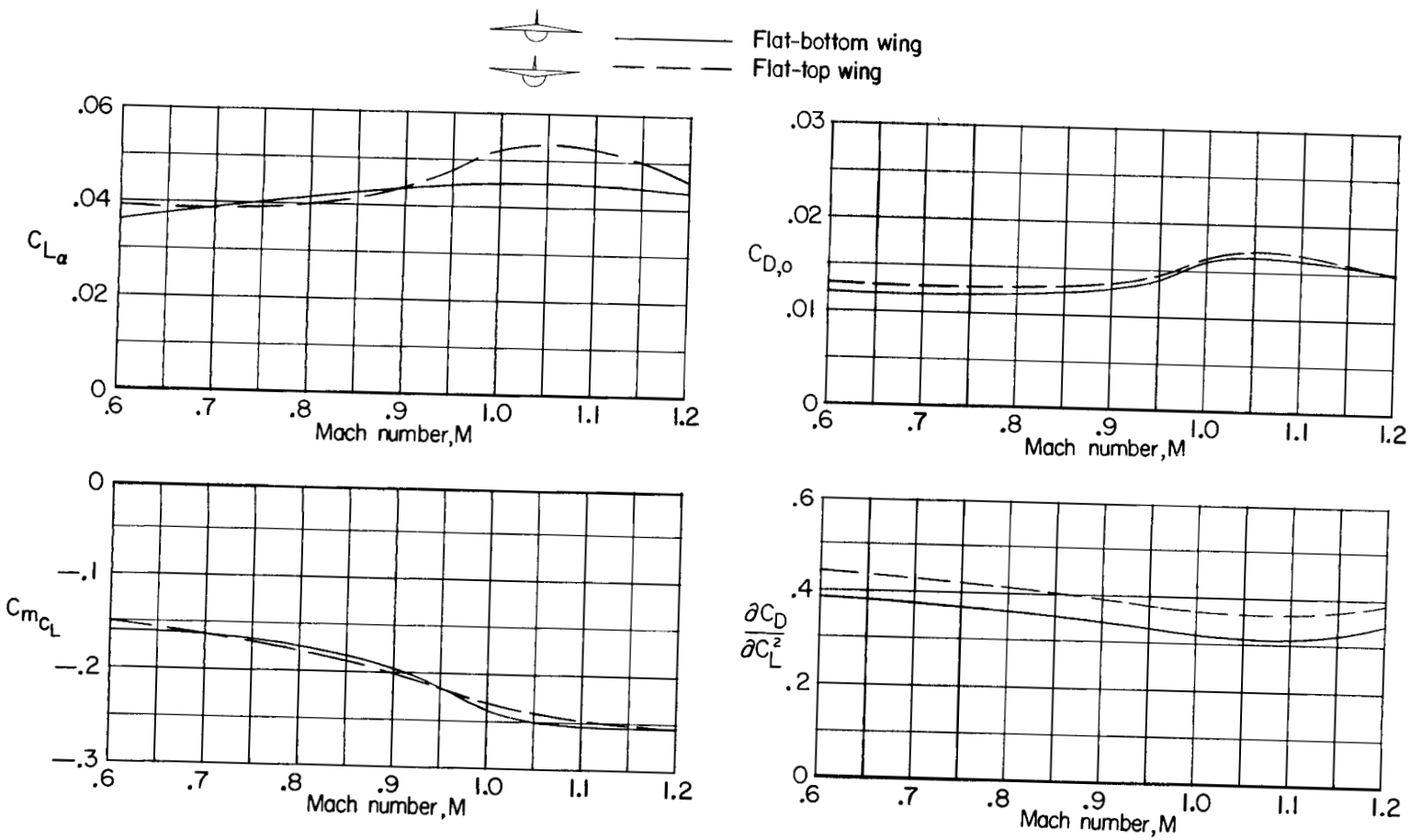


(a) High-wing arrangement.

Figure 10.- Effect of wing section and wing arrangement on the longitudinal-stability and drag parameters.

UNCLASSIFIED

UNCLASSIFIED

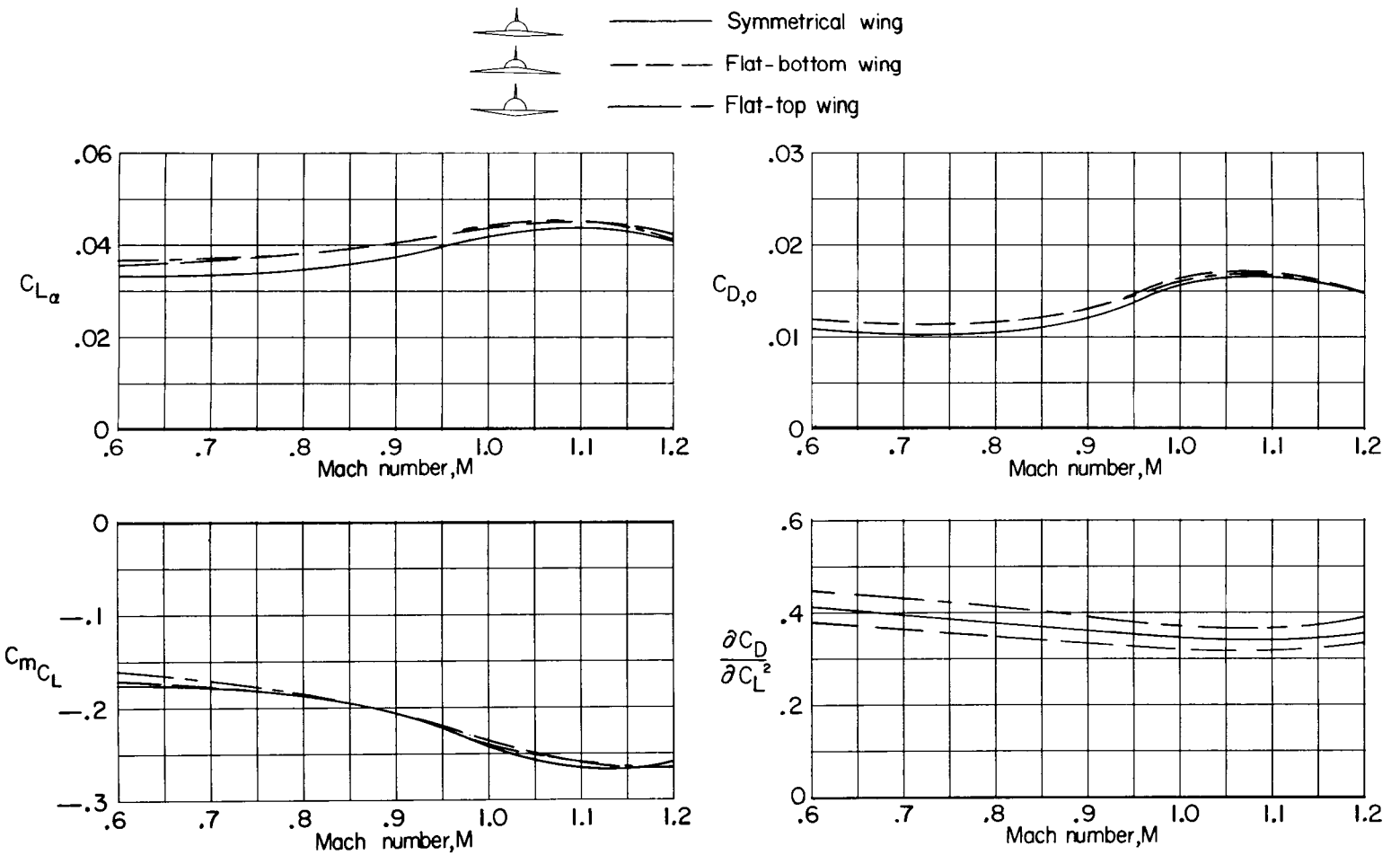


(b) Low-wing arrangement.

Figure 10.- Concluded.

UNCLASSIFIED

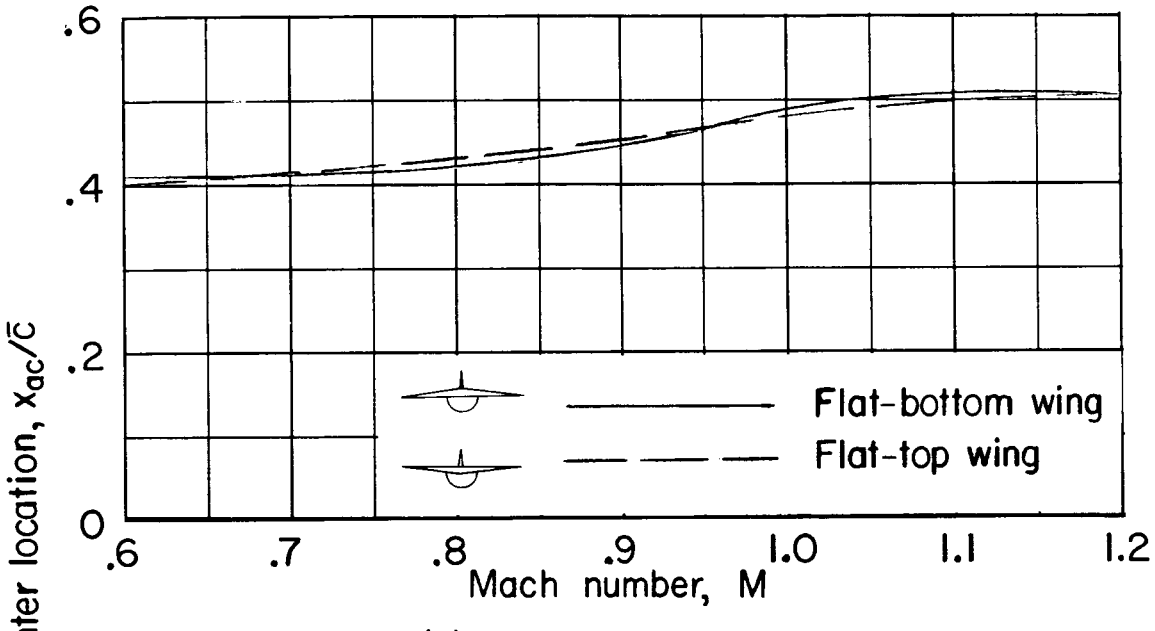


(a) High-wing arrangement.

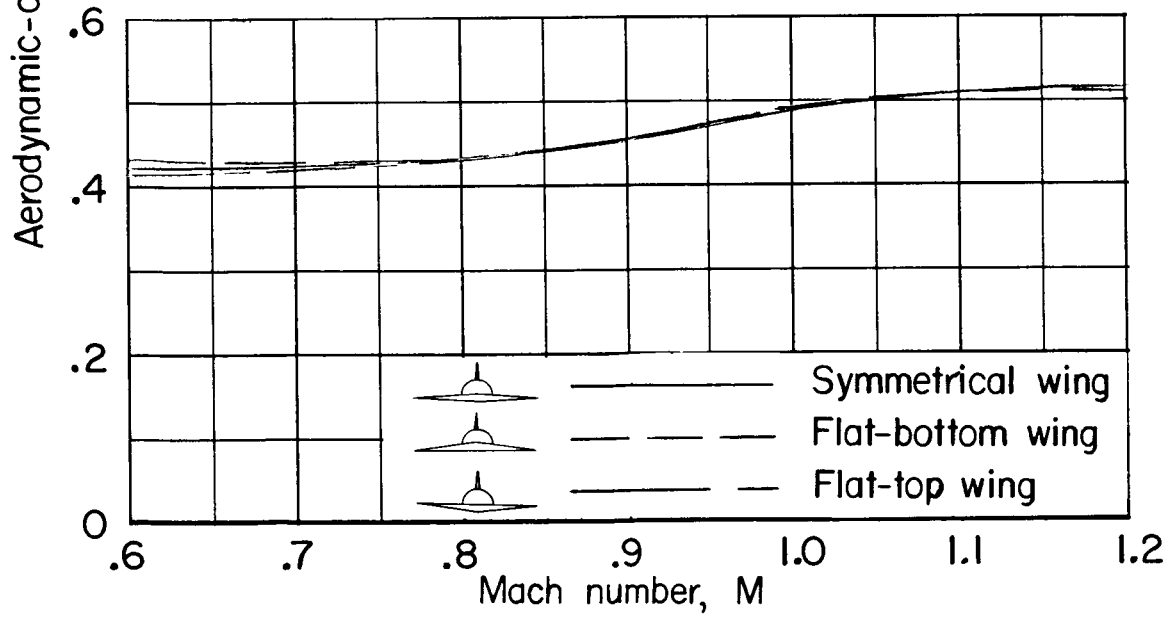


(b) Low-wing arrangement.

Figure 11.- Effect of wing section and wing arrangement on the variation of aerodynamic-center location with Mach number.

UNCLASSIFIED [redacted]

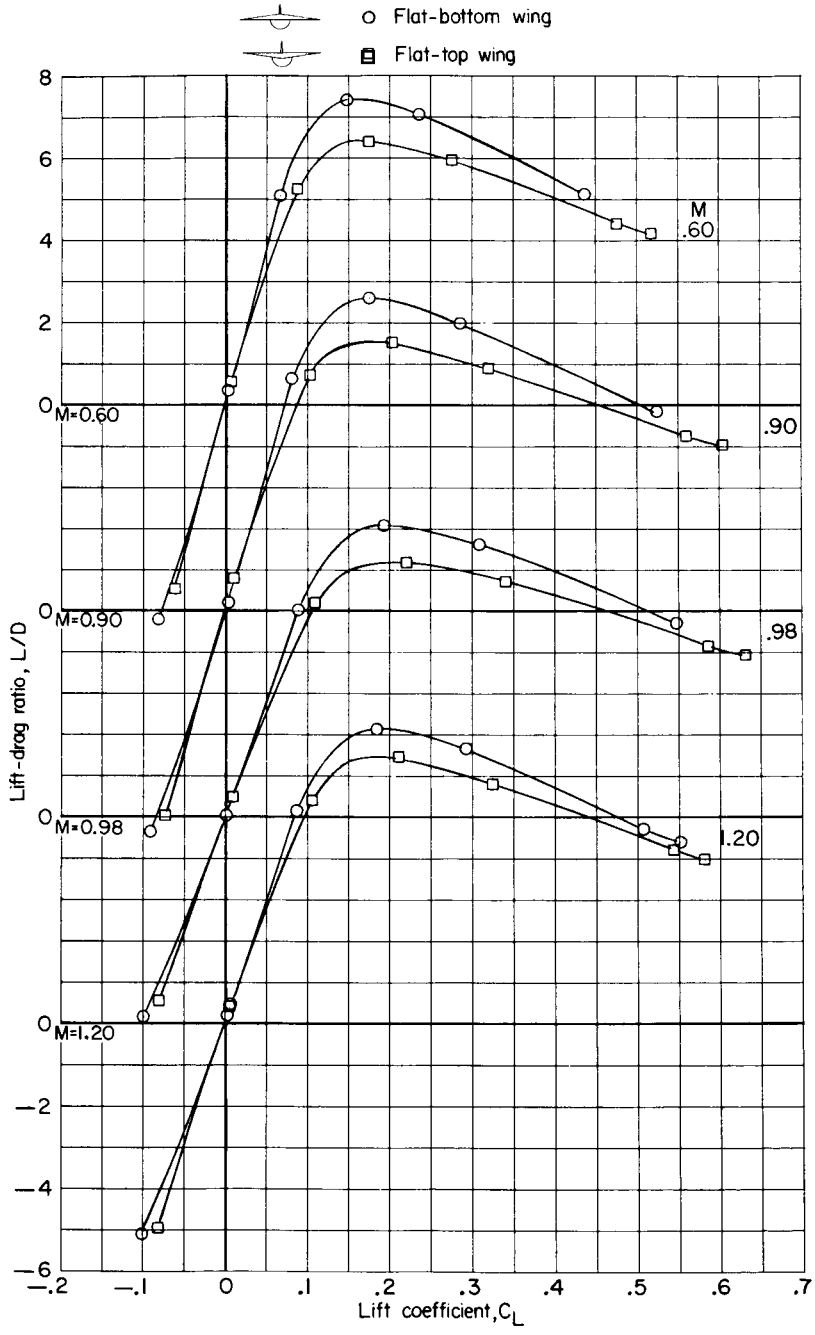


(a) High-wing arrangement.

Figure 12.- Effect of wing section and wing arrangement on the variation of L/D with lift coefficient.

UNCLASSIFIED [redacted]

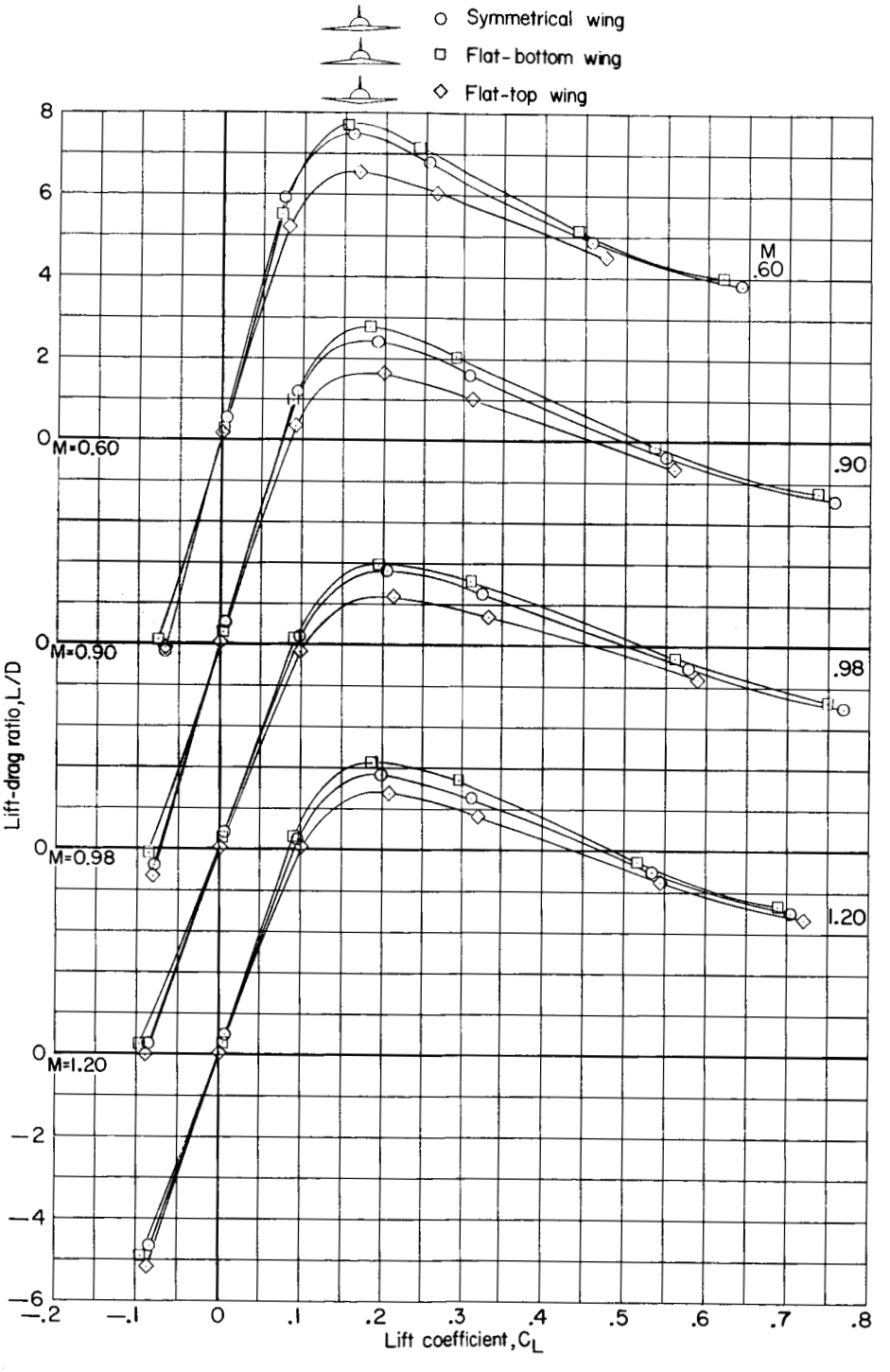


(b) Low-wing arrangement.

Figure 12.- Concluded.

UNCLASSIFIED

[redacted]

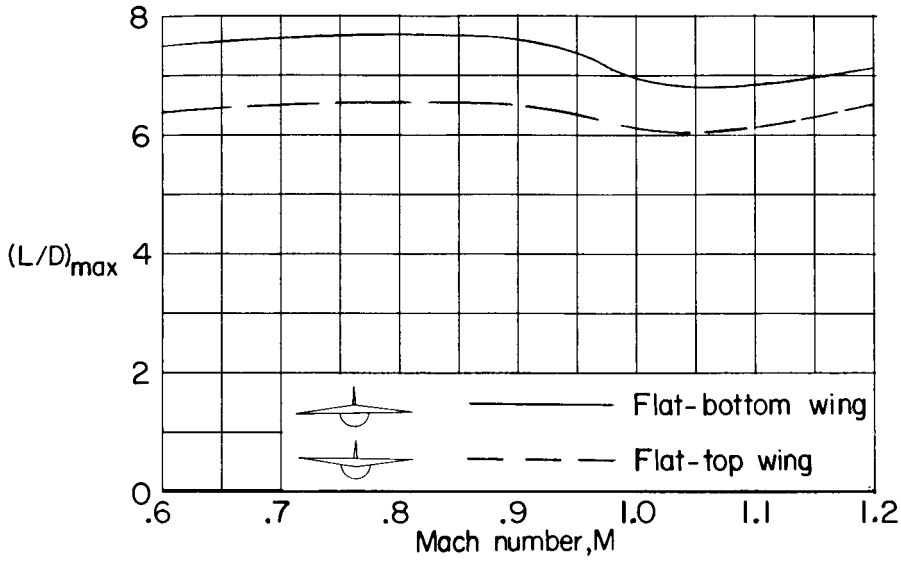


(a) High-wing arrangement.

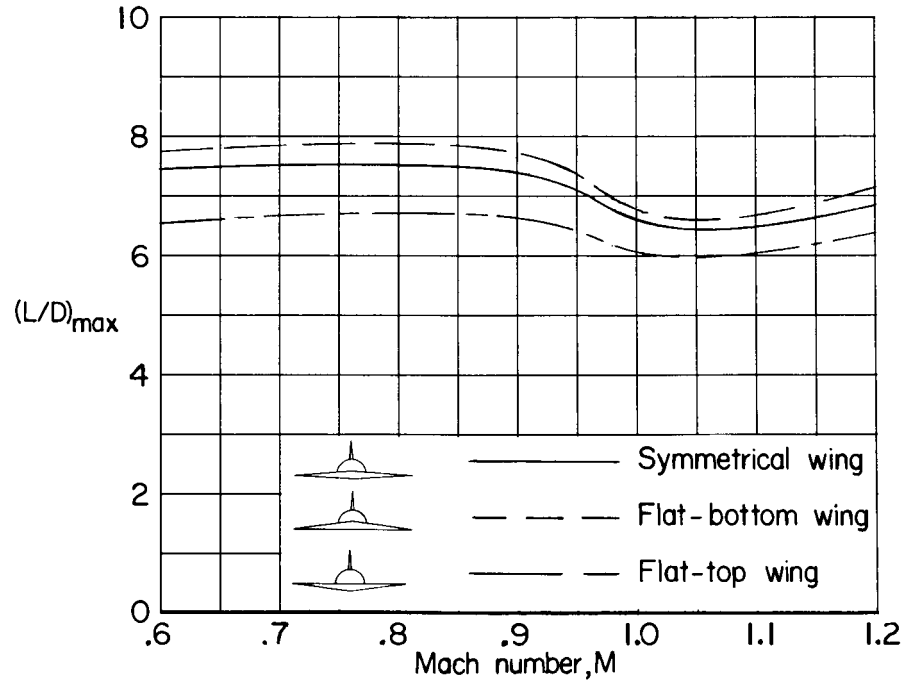


(b) Low-wing arrangement.

Figure 13.- Effect of wing section and wing arrangement on the variation of $(L/D)_{max}$ with Mach number.

UNCLASSIFIED [redacted]

L-1975

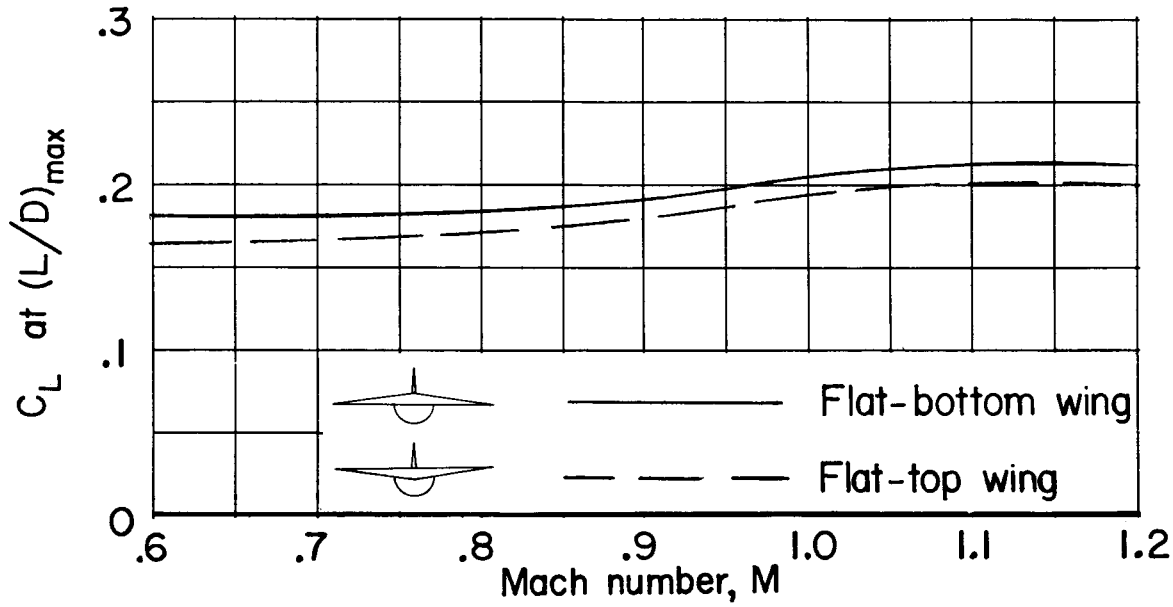


(a) High-wing arrangement.

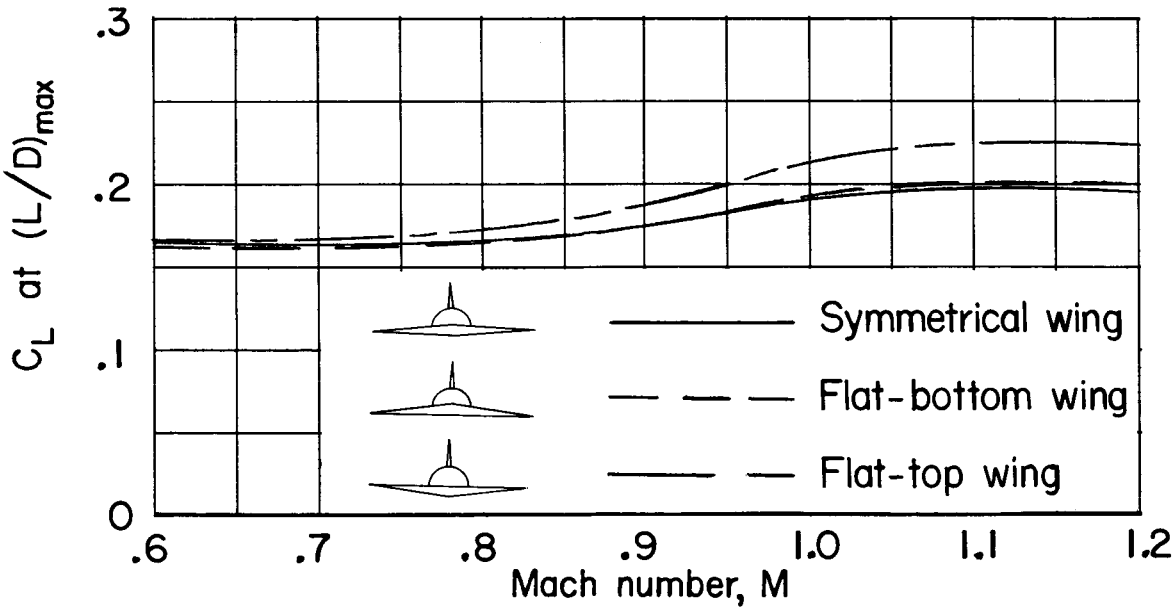


(b) Low-wing arrangement.

Figure 14.- Effect of wing section and wing arrangement on the variation of lift coefficient for $(L/D)_{max}$ with Mach number.

UNCLASSIFIED
[redacted]

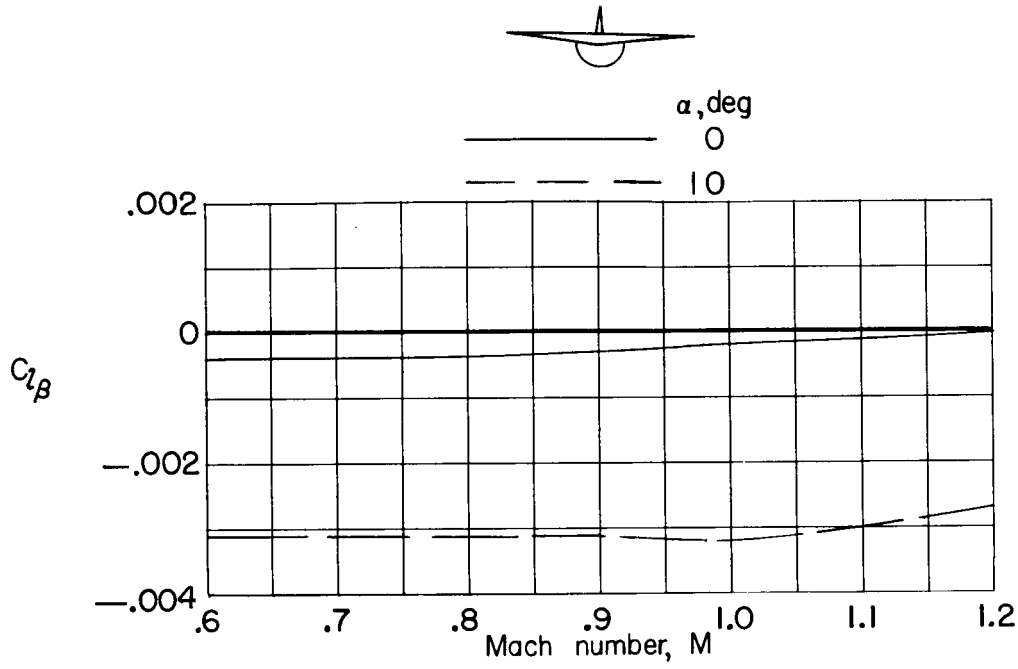


(a) Effective-dihedral parameter plotted against Mach number.

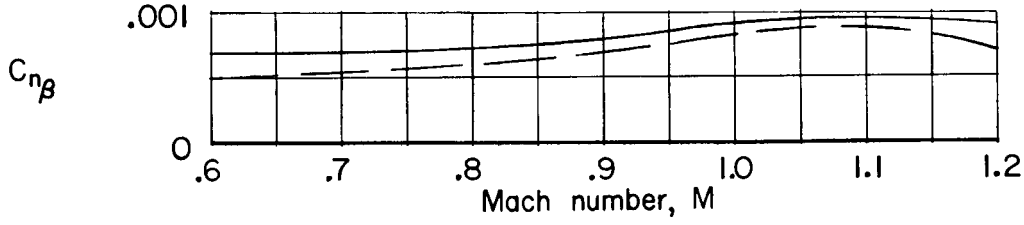


(b) Directional-stability parameter plotted against Mach number.

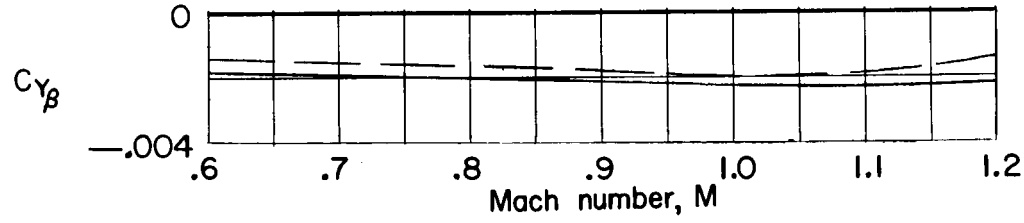


(c) Lateral-force parameter plotted against Mach number.

Figure 15.- Effect of angle of attack on the variation of the lateral-directional-stability parameters with Mach number for the high-wing arrangement with flat-top wing.

L-1975

UNCLASSIFIED
[redacted]

[redacted]

UNCLASSIFIED

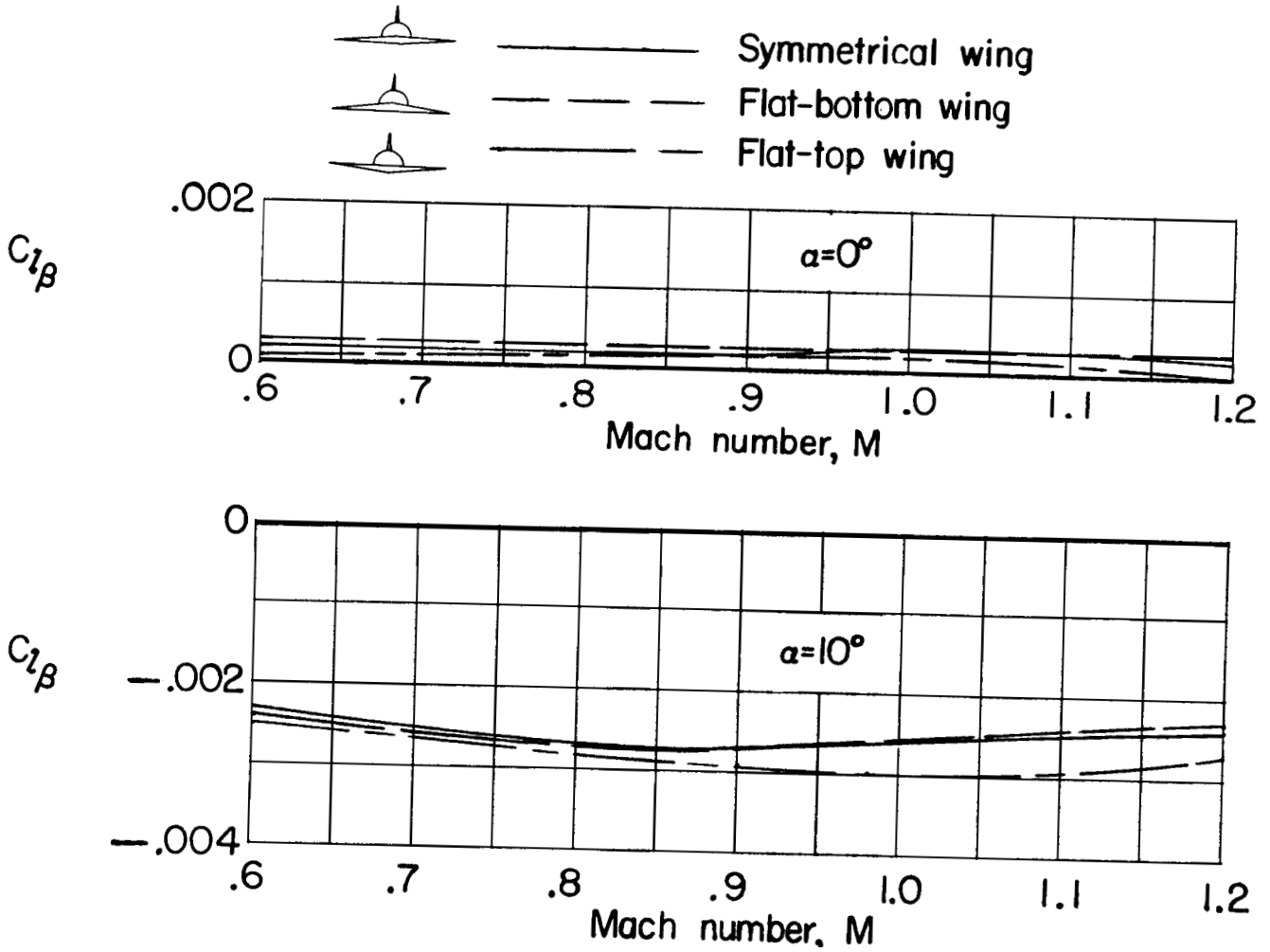


(a) Effective-dihedral parameter plotted against Mach number.

Figure 16.- Effect of wing section and angle of attack on the variation of the lateral-directional-stability parameters with Mach number for the low-wing arrangement.

[redacted]

UNCLASSIFIED

UNCLASSIFIED

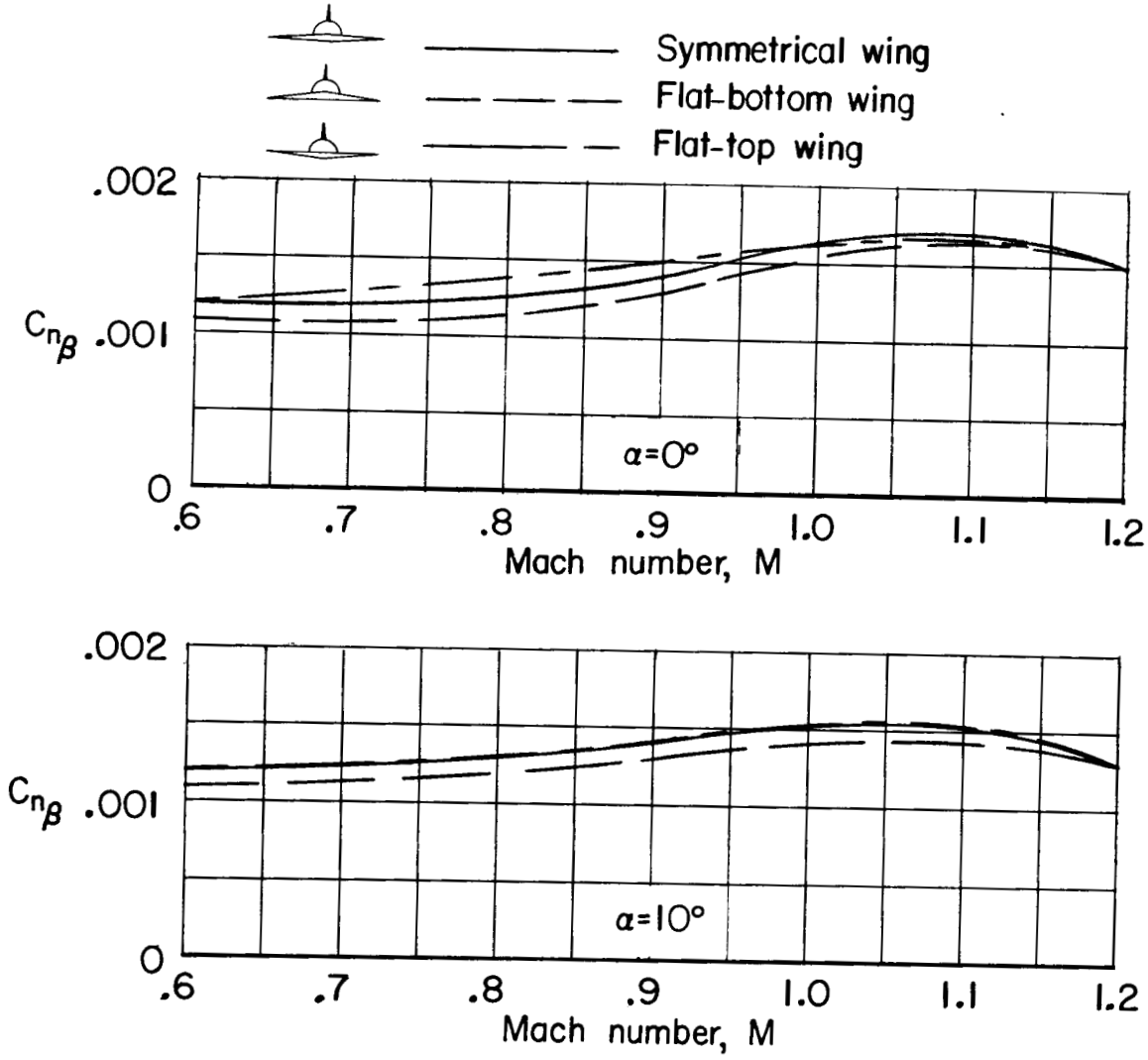


(b) Directional-stability parameter plotted against Mach number.

Figure 16.- Continued.

UNCLASSIFIED

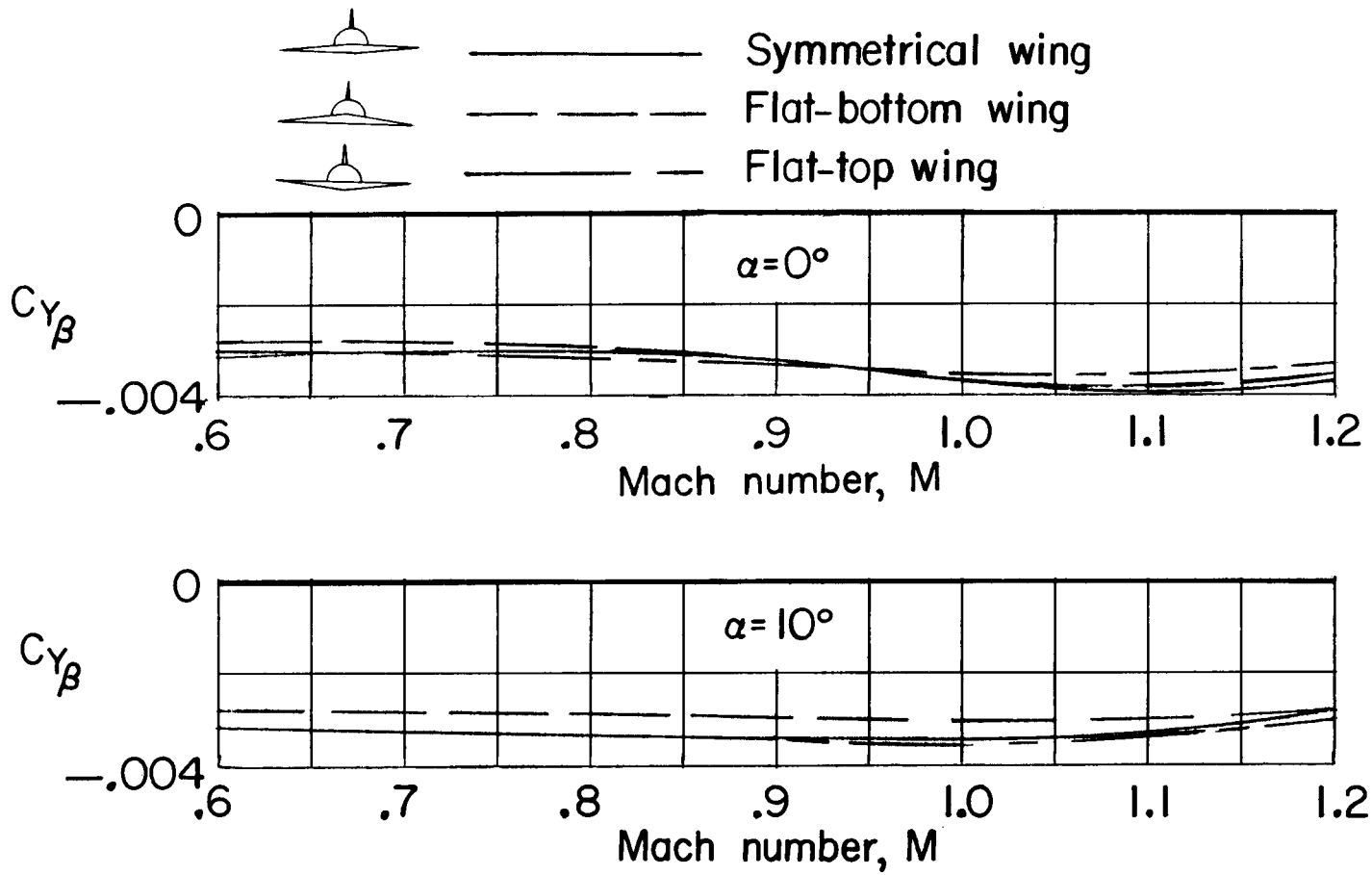


(c) Side-force parameter plotted against Mach number.

Figure 16.- Concluded.

UNCLASSIFIED
[redacted]
UNCLASSIFIED



NASA-Langley, 1962 L-1975

[redacted]
UNCLASSIFIED